normal dG:dC base pair. Calf thymus Polα incorporates 8-oxo-dGTP opposite dC with a F_{inc} of less than 10^{-5} [57]. The B-family Pols involved in chromosome replication appear to be highly resistant to mutations induced by the incorporation of 8-oxo-dGTP into DNA. An exception may be Polζ because knocking down the expression of *POLZ*, which encodes Polζ, in human cells significantly reduces mutations induced by 8-oxo-dGTP [58]. The Pol may be involved in an extension step from 8-oxo-dG:dA mismatch after the incorporation of 8-oxo-dGTP opposite template dA by other Pols, as suggested for TLS.

B-family Pols in other species also incorporate 8-oxo-dGTP inefficiently. Archaea *Sulfolobus solfataricus Sso* Pol B1 is a replicase that incorporates 8-oxo-dGTP ineffectively [59] and slightly more often opposite template dC than template dA (Table 2). *E. coli* Pol II exo⁻ is the most inefficient enzyme examined thus far for the incorporation of 8-oxo-dGTP into DNA ($F_{inc} = 3.1 \times 10^{-6}$) and it has a preference for template dC [41].

2.3. C-family Pols

C-family Pols are homologues of the α subunit of *E. coli* Pol III holoenzyme, which is responsible for the replication of the *E. coli* genome [43]. *E. coli* Pol III holoenzyme is composed of the core (α, β and θ), γ complex, and β subunit. The core is a heterotrimer of the α Pol (catalytic subunit), ε subunit with 3′ to 5′ proofreading exonuclease, and θ subunit. The β subunit is a sliding clamp, which encircles duplex DNA and increases processivity, and the γ complex is the clamp loader. The C-family Pols are exclusively found in eubacteria, whereas all Archaea and eukaryotic replicative Pols belong to the B family. Although Pol III is responsible for replication in this organism, the α subunit of Pol III efficiently incorporates 8-oxo-dGTP opposite both dA and dC ($F_{inc} = 3.9 \times 10^{-2}$) [28]. This F_{inc} is substantially higher than the replicative Pols belonging to the A and B families (Table 1), which may be due to the structural resemblance of the α subunit to X-family Pols [60,61] (see more detail below). The probability that 8-oxo-dGTP is incorporated into DNA during *E. coli* replication may be higher compared to mammalian cells. *E. coli* Pol III holoenzyme lacking the β subunit is referred to as Pol III*. Unlike the α subunit, Pol III* tends to incorporate 8-oxo-dGTP opposite template dA more often than template dC (Yamada, et al., unpublished data). Complex formation with other subunits may alter the enzyme's template base preference. In addition to 8-oxo-dGTP, Pol III holoenzyme also incorporates 2-OH-dATP, an oxidized form of dATP, which induces a G:C to T:A transversion when it is incorporated opposite template dG [62].

2.4. X-family Pols

In humans, Polβ, Polλ, Polσ, Polμ, and terminal deoxynucleotidyl transferase (TdT) belong to the X family of Pols [63]. Because these Pols are involved in short DNA synthesis for repair rather than long DNA synthesis for chromosome replication, the family was termed X to differentiate from the A, B, and C families. Polβ plays important roles in gap-filling synthesis in base excision repair, and Polλ may have functions similar to Polβ [64–66]. Polλ also contributes to non-homologous end joining in the process of repairing double-strand DNA breaks [67]. Polβ and Polλ exhibit relatively high F_{inc} values when they incorporate 8-oxo-dGTP into gapped DNA (Fig. 1 and Table 1) [68,69]. In particular, Polβ incorporates 8-oxo-dGTP with an efficiency roughly 20% of that of normal dNTP incorporation. Both Pols prefer dA as a template base for incorporating 8-oxo-dGTP (Table 1). The priority of the enzymes may be the execution of DNA synthesis for repair rather than the exclusion of 8-oxo-dGTP from DNA to maintain genomic integrity. Among X-family Pols, Pol X from African swine fever virus

(ASFV) prefers template dC for the incorporation of 8-oxo-dGTP [70].

2.5. Y-family Pols

The most remarkable feature of this family is the ability to bypass a variety of lesions in DNA that otherwise block chromosome replication by A-, B-, and C-family Pols [51,55,71]. Because the enzymes are involved in short track DNA synthesis rather than long DNA synthesis for chromosome replication, they are termed the Y family, following the X family. In general, these enzymes have large active sites to accommodate bulky lesions in DNA and lack 3′ to 5′ exonuclease activities [72]. The fidelity of DNA synthesis by Y-family Pols is much lower compared to that of replicative A-, B-, and C-family Pols [42]. In humans, Y-family Pols include REV1, Polη, Polκ, and Polι. Like Polβ in the X family, Polη, Polκ, and Polι efficiently incorporate 8-oxo-dGTP into DNA and favor dA as the template base. In particular, Polη exhibits the highest F_{inc} of 20–60% (Table 1), suggesting that it incorporates 8-oxo-dGTP opposite template dA almost as much as it incorporates dTTP into DNA [39,40]. Therefore, Y-family Pols seem to incorporate 8-oxo-dGTP into the cellular DNA efficiently although they have fewer chances to incorporate the oxidized nucleotide compared to the replicative Pols. Interestingly, suppressed expression of Polη and REV1 by siRNAs significantly reduces mutations in the *supF* plasmid in human cells in which 8-oxo-dGTP is introduced by osmotic shock [58]. In addition to 8-oxo-dGTP, Polη incorporates 2-OH-dATP opposite template T, G, and C with an efficiency of 2–6% of that of incorporating normal dNTPs [40]. In bacteria and Archaea, the Y-family Pols Pol IV (DinB) in *E. coli* and Dbh (*Sac* Pol Y1) and Dpo4 (*Sso* Pol Y1) in Archaea also incorporate 8-oxo-dGTP efficiently, favoring dA as the template base for incorporation [48,59]. Deficient *dinB* and/or *umu* expression (encoding Pol IV and Pol V, respectively), reduces the mutation frequency of A:T to C:G by 80–90% in *sod fur E. coli* mutants in which iron overload and superoxide stress occur [48]. The Y-family Pols in *E. coli* may be involved in the transversion mutations caused by 8-oxo-dGTP under SOS-induced conditions, and they may participate in sequential biochemical steps, such as the incorporation and extension of 8-oxo-dGTP during chromosome replication. *E. coli* Pol IV and Pol V appear to be involved in chromosome replication when the dNTP pool is depleted by treating the cells with hydroxyurea [73]. Whether the Pols incorporate 8-oxo-dGTP into DNA when they are involved in chromosome replication is of interest.

3. Structural insight into the template base preference by polymerases for incorporating 8-oxo-dGTP into DNA

The 8-oxo-dG molecule mainly exists in a 6,8-diketo form in solution at physiological pH, and its conformation is in equilibrium between the *anti* and *syn* formation, with the *syn* conformation being energetically favored [13–15,74]. Therefore, 8-oxo-dGTP is expected to pair with template dA more favorably than template dC. However, as described above, the template base preferred by Pols is significantly different, even in the same family (Table 2). This difference suggests that the sterical and/or electrostatic properties of the active site of Pols play important roles in the conformation of 8-oxo-dGTP in the enzyme where it pairs with template bases. Indeed, studies have indicated that particular amino acids in the active site greatly impact specificity for the incorporation of 8-oxo-dGTP into DNA by affecting the conformation of 8-oxo-dGTP in the active site.

In Polβ in humans, Asn 279 (N279) is the critical determinant of template base preference for incorporating 8-oxo-dGTP [68]. Wild-type Polβ exhibits a preference for template dC over template dA

at a ratio of 24:1 when it incorporates 8-oxo-dGTP. However, the mutant enzyme with alanine instead of N279 displays a reversed preference. The mutant (N279A) incorporates 8-oxo-dGTP opposite template dC and dA at a ratio of 14:1. The N279 appears to form a hydrogen bond with the O^8 of incoming 8-oxo-dGTP in the syn formation, which stabilizes the formation of 8-oxo-dGTP:dA (Fig. 2A). The active site of Polβ may alter the equilibrium of the conformation of 8-oxo-dGTP through interactions with N279.

φ29 Pol generally favors template dC for the insertion of 8-oxo-dGTP [56]; the ratio of pairing dA to 8-oxo-dGTP compared to pairing dC is 1:3. Structural modeling based on the crystal structure of the RB69 Pol active site suggests that this specificity is dominated by Lys 383 (K383), which sterically and/or electrostatically impinges the N^2 of 8-oxo-dGTP in the syn formation when paired with dA, thereby forcing it to form the anti conformation (Fig. 2B).

Human Y-family Pols, i.e., Polκ and Polη, have other mechanisms for selecting 8-oxo-dGTP [39]. In human Polκ, which exclusively incorporates 8-oxo-dGTP opposite template dA, the substitution of Tyr112 (Y112) with alanine eliminates the preference, mainly due to severely reduced efficiency for pairing with template dA (270-fold reduction) compared to that of pairing with template dC (15-fold reduction). Thus, the ratio of dA to dC for pairing with 8-oxo-dGTP is reduced from 11:1 to almost 1:1 by the amino acid substitution. Y112 is known as the 'steric gate', which distinguishes dNTPs from rNTPs by sensing the absence of the ribose 2′-hydroxy group. In addition, the residue is involved in an incorporation step of dCTP opposite a benzo[a]pyrene 7,8-dihydrodiol 9,10-epoxide-N^2-dG adduct in the template DNA and an extension step from mismatched termini [75]. Therefore, Y112 in human Polκ has multiple functions and may interact with both the sugar moiety and the base of the incoming dNTP, as well as stabilize the pairing of template dA with 8-oxo-dGTP in the syn conformation in the active site.

In contrast, phenylalanine 18 (F18) of human Polη, which corresponds to Y112 in human Polκ, does not affect the template base preferred by this Y-family Pol [39]. An amino acid substitution of F18 with alanine does not alter the enzyme's specificity for incorporating 8-oxo-dGTP into DNA; instead, arginine 61 (R61) affects the preference. Human Polη incorporates 8-oxo-dGTP opposite template dA almost exclusively. However, substitutions of R61 with alanine (R61A) or lysine (R61K) drastically alter the template base preference. The ratio of incorporation of 8-oxo-dGTP opposite template dA versus dC is 660:1 for the wild-type Pol, 65:1 for R61A, and 7:1 for R61K. Similar alterations in the template base prefer-
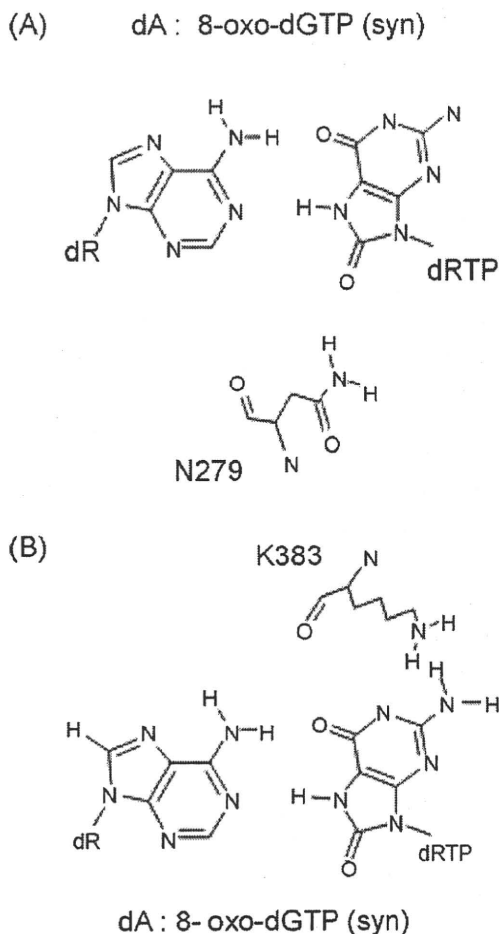

Fig. 2. Schematic representation of amino acids affecting the pairing of dA:8-oxo-dGTP(syn). (A) In hPolβ, a hydrogen bond can be present between NH₂ of N279 and the O^8 of 8-oxo-dGTP in the syn conformation. (B) In φ29 Pol, sterical and/or electrostatic collisions could occur between K383 and the N^2 of 8-oxo-dGTP in the syn conformation. The collision may force 8-oxo-dGTP to form the anti conformation in the active site.
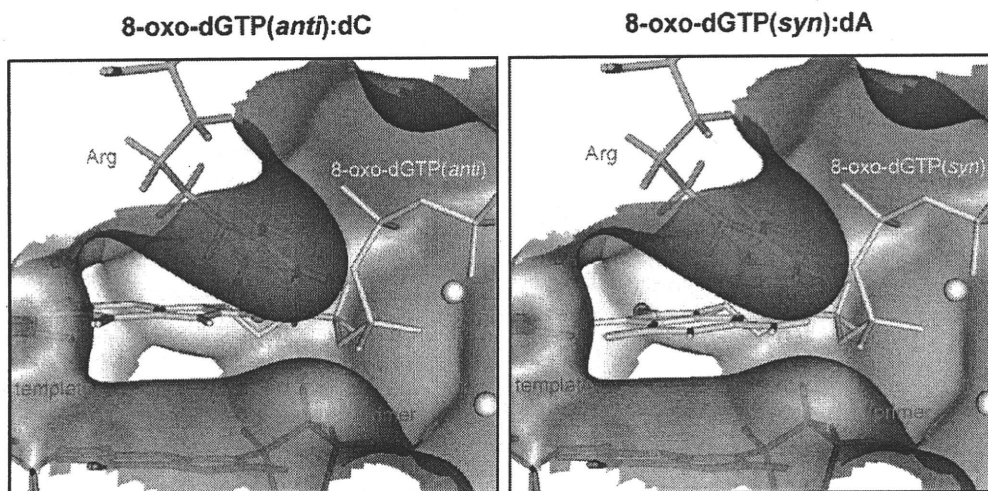

Fig. 3. The modeling structures of 8-oxo-dGTP(anti):dC and 8-oxo-dGTP(syn):dA in the active site of hPolη. R61 (ocher) may sterically clash with the O^8 of the incoming 8-oxo-dGTP in the anti conformation, leading to the exclusion of a pairing with template dC.

ence occur in the case of 8-oxo-dATP but not 2-OH-dATP. Molecular modeling studies suggest that R61 causes steric and/or electrostatic hindrance with the O^8 of 8-oxo-dGTP and 8-oxo-dATP in the *anti* conformation (Fig. 3). This context may be the basis for the preference of human Polη for pairing 8-oxo-dGTP with template dA. When R61 is replaced by lysine, the ε-amino group and O^8 of 8-oxo-dGTP in the *anti* conformation may interact electrostatically. Thus, the lysine residue (K61), but not the arginine residue (R61), may stabilize 8-oxo-dGTP in the *anti* conformation, which enhances the preference for correctly pairing 8-oxo-dGTP with template dC. The counterpart of R61 in yeast Polη is R73, which is involved in bypass reactions across 1,2-(GpG) cisplatin adducts in DNA [76].

4. Biological implications of incorporation of oxidized dNTPs into DNA by Pols

The incorporation of 8-oxo-dGTP into DNA opposite template dA may cause mutations because the incorporated 8-oxo-dG can pair with dCTP in the next round of DNA replication, thereby inducing A:T to C:G transversions. Reasonably, A- and B-family Pols, most of which are involved in chromosome replication, incorporate 8-oxo-dGTP into DNA inefficiently and most disfavor the pairing of 8-oxo-dGTP with template dA (Fig. 1 and Table 1). The eukaryotic genome may be dually protected from the mutagenic threats of 8-oxo-dGTP incorporation into DNA by the presence of MTH1 and other sanitizing enzymes that hydrolyze oxidized nucleotides, and by the poor ability of the Pols to incorporate the oxidized nucleotides into DNA.

In contrast, the C-family Pols, such as *E. coli* Pol III (both the assembled holoenzyme, Pol III*, and the catalytic α-subunit alone), have high activity for incorporating 8-oxo-dGTP into DNA and pairs it with template dA rather than dC (Tables 1 and 2). The enzyme incorporates the oxidized dNTP opposite template dA at approximately 4% of the efficiency of incorporating the normal dTTP opposite template dA [28]. The high efficiency of incorporating 8-oxo-dGTP opposite dA may account for the extremely high mutation frequency of the *mutT E. coli* mutants in which A:T to C:G transversion mutations are increased more than 1000 times over the wild-type strain. In this respect, the bacterial genome is less protected from the mutagenic effect of 8-oxo-dGTP compared to eukaryotes, which may be due to the structural similarity of the α-subunit of Pol III to Polβ in family X rather than replicative Pols in family A or B [60,61,77]. The structure of the palm domain of the α-subunit of *Thermus aquaticus* Pol III is similar to that of the palm domain of rat Polβ [60]. The amino acid sequence of the α-subunit of *T. aquaticus* is roughly 40% identical to that of the *E. coli* homologue. A large fragment of the α-subunit of *E. coli* Pol III is partly similar to the catalytic domain of Polβ [61]. However, whether the efficient incorporation of 8-oxo-dGTP by *E. coli* Pol III is achieved by mechanisms similar to those in Polβ remains unknown.

The X- and Y-family Pols also efficiently incorporate 8-oxo-dGTP and prefer template dA. In particular, human Polβ and Polη have the pair 8-oxo-dGTP with dA comparable to dTTP with dA [39,40,68]. The enzymes may incorporate 8-oxo-dGTP into DNA at a high frequency and cause A:T to C:G transversions. The erroneous incorporation of 8-oxo-dGTP opposite template dA may be analogous to the error-prone TLS by the Y-family Pols because two pathways enhance the induction of mutations during DNA synthesis.

5. Future perspective

Most of Pols seem to share a common architecture with three domains, the fingers, palm, and thumb, although Y-family Pols have an extra little finger domain, which is also called the polymerase-associated domain (PAD) or wrist domain [72,78–80]. The fingers interact with incoming dNTPs and the single-stranded template DNA, the palm holds two catalytic metals, and the thumb binds duplex DNA. Despite the structural similarities, Pols have remarkably divergent properties for the incorporation of 8-oxo-dGTP into DNA. In addition, the mechanism underlying the erroneous incorporation of 8-oxo-dGTP opposite template dA is distinct among φ29 Pol, human Polβ, human Polκ, and human Polη, suggesting the convergent evolution of Pols to incorporate the mutagenic oxidized nucleotide into DNA. The biological or evolutionary merits of the efficient incorporation of 8-oxo-dGTP opposite template dA are of great interest. In addition, it is worth investigating how accessory factors such as PCNA/RFA affect the efficiency and template preference of Pols [81,82]. Erroneous TLS or error-prone Pols have been proposed to be needed to adequately adapt to environmental changes during evolution [83]. Similarly, the incorporation of 8-oxo-dGTP, and perhaps other oxidized dNTPs, into DNA may have be advantageous in competition with other organisms during evolution, though it is harmful for multicellular organisms, such as humans, maintaining their genomic integrity and longevity.

Conflict of interest

No conflicting interest exists.

References

[1] T. Lindahl, Instability and decay of the primary structure of DNA, Nature 362 (1993) 709–715.
[2] M. Dizdaroglu, Chemical determination of free radical-induced damage to DNA, Free Radic. Biol. Med. 10 (1991) 225–242.
[3] A.L. Jackson, L.A. Loeb, The contribution of endogenous sources of DNA damage to the multiple mutations in cancer, Mutat. Res. 477 (2001) 7–21.
[4] R.A. Floyd, Measurement of oxidative stress in vivo, in: K.J.A. Daview, F. Ursini (Eds.), The Oxygen Paradox, Cleup University Press, Cleup, 1995, pp. 89–103.
[5] M. Dizdaroglu, Mechanisms of oxidative damage: lesions and their measurement, in: M. Dizdaroglu, A. Karakaya (Eds.), Advances in DNA Damage and Repair, Kluwer Academic Publishers/Plenum Press, New York, 1999, pp. 67–87.
[6] Y.Z. Fang, S. Yang, G. Wu, Free radicals, antioxidants, and nutrition, Nutrition 18 (2002) 872–879.
[7] B.N. Ames, Dietary carcinogens and anticarcinogens. Oxygen radicals and degenerative diseases, Science 221 (1983) 1256–1264.
[8] D.I. Feig, T.M. Reid, L.A. Loeb, Reactive oxygen species in tumorigenesis, Cancer Res. 54 (1994) 1890s–1894s.
[9] H. Kasai, Chemistry-based studies on oxidative DNA damage: formation, repair, and mutagenesis, Free Radic. Biol. Med. 33 (2002) 450–456.
[10] M.L. Michaels, J.H. Miller, The GO system protects organisms from the mutagenic effect of the spontaneous lesion 8-hydroxyguanine (7,8-dihydro-8-oxoguanine), J. Bacteriol. 174 (1992) 6321–6325.
[11] H. Kasai, S. Nishimura, Hydroxylation of deoxyguanosine at the C-8 position by ascorbic acid and other reducing agents, Nucleic Acids Res. 12 (1984) 2137–2145.
[12] T.A. Kunkel, The high cost of living, in: American Association for Cancer Research Special Conference: Endogenous Sources of Mutations, Fort Myers, Florida, USA, 11–15 November 1998, Trends Genet. 15 (1999) 93–94.
[13] M. Kouchakdjian, V. Bodepudi, S. Shibutani, M. Eisenberg, F. Johnson, A.P. Grollman, D.J. Patel, NMR structural studies of the ionizing radiation adduct 7-hydro-8-oxodeoxyguanosine (8-oxo-7H-dG) opposite deoxyadenosine in a DNA duplex. 8-Oxo-7H-dG(syn).dA(anti) alignment at lesion site, Biochemistry 30 (1991) 1403–1412.

[14] Y. Oda, S. Uesugi, M. Ikehara, S. Nishimura, Y. Kawase, H. Ishikawa, H. Inoue, E. Ohtsuka, NMR studies of a DNA containing 8-hydroxydeoxyguanosine, Nucleic Acids Res. 19 (1991) 1407–1412.

[15] L.A. Lipscomb, M.E. Peek, M.L. Morningstar, S.M. Verghis, E.M. Miller, A. Rich, J.M. Essigmann, L.D. Williams, X-ray structure of a DNA decamer containing 7,8-dihydro-8-oxoguanine, Proc. Natl. Acad. Sci. USA 92 (1995) 719–723.

[16] S. Shibutani, M. Takeshita, A.P. Grollman, Insertion of specific bases during DNA synthesis past the oxidation-damaged base 8-oxodG, Nature 349 (1991) 431–434.

[17] K.C. Cheng, D.S. Cahill, H. Kasai, S. Nishimura, L.A. Loeb, 8-Hydroxyguanine, an abundant form of oxidative DNA damage, causes G–T and A–C substitutions, J. Biol. Chem. 267 (1992) 166–172.

[18] T. Nohmi, S.R. Kim, M. Yamada, Modulation of oxidative mutagenesis and carcinogenesis by polymorphic forms of human DNA repair enzymes, Mutat. Res. 591 (2005) 60–73.

[19] H. Ide, M. Kotera, Human DNA glycosylases involved in the repair of oxidatively damaged DNA, Biol. Pharm. Bull. 27 (2004) 480–485.

[20] H. de Waard, J. de Wit, J.O. Andressoo, C.T. van Oostrom, B. Riis, A. Weimann, H.E. Poulsen, H. van Steeg, J.H. Hoeijmakers, G.T. van der Horst, Different effects of CSA and CSB deficiency on sensitivity to oxidative DNA damage, Mol. Cell Biol. 24 (2004) 7941–7948.

[21] M. D'Errico, E. Parlanti, M. Teson, P. Degan, T. Lemma, A. Calcagnile, I. Iavarone, P. Jaruga, M. Ropolo, A.M. Pedrini, D. Orioli, G. Frosina, G. Zambruno, M. Dizdaroglu, M. Stefanini, E. Dogliotti, The role of CSA in the response to oxidative DNA damage in human cells, Oncogene 26 (2007) 4336–4343.

[22] J. Tuo, P. Jaruga, H. Rodriguez, V.A. Bohr, M. Dizdaroglu, Primary fibroblasts of Cockayne syndrome patients are defective in cellular repair of 8-hydroxyguanine and 8-hydroxyadenine resulting from oxidative stress, FASEB J. 17 (2003) 668–674.

[23] Y. Homma, M. Tsunoda, H. Kasai, Evidence for the accumulation of oxidative stress during cellular ageing of human diploid fibroblasts, Biochem. Biophys. Res. Commun. 203 (1994) 1063–1068.

[24] T. Kaneko, S. Tahara, T. Taguchi, H. Kondo, Accumulation of oxidative DNA damage, 8-oxo-2′-deoxyguanosine, and change of repair systems during in vitro cellular aging of cultured human skin fibroblasts, Mutat. Res. 487 (2001) 19–30.

[25] I. Schmerold, H. Niedermuller, Levels of 8-hydroxy-2′-deoxyguanosine in cellular DNA from 12 tissues of young and old Sprague–Dawley rats, Exp. Gerontol. 36 (2001) 1375–1386.

[26] T. Lu, Y. Pan, S.Y. Kao, C. Li, I. Kohane, J. Chan, B.A. Yankner, Gene regulation and DNA damage in the ageing human brain, Nature 429 (2004) 883–891.

[27] M. Sekiguchi, T. Tsuzuki, Oxidative nucleotide damage: consequences and prevention, Oncogene 21 (2002) 8895–8904.

[28] H. Maki, M. Sekiguchi, MutT protein specifically hydrolyses a potent mutagenic substrate for DNA synthesis, Nature 355 (1992) 273–275.

[29] T. Tsuzuki, A. Egashira, H. Igarashi, T. Iwakuma, Y. Nakatsuru, Y. Tominaga, H. Kawate, K. Nakao, K. Nakamura, F. Ide, S. Kura, Y. Nakabeppu, M. Katsuki, T. Ishikawa, M. Sekiguchi, Spontaneous tumorigenesis in mice defective in the MTH1 gene encoding 8-oxo-dGTPase, Proc. Natl. Acad. Sci. USA 98 (2001) 11456–11461.

[30] P. Rai, T.T. Onder, J.J. Young, J.L. McFaline, B. Pang, P.C. Dedon, R.A. Weinberg, Continuous elimination of oxidized nucleotides is necessary to prevent rapid onset of cellular senescence, Proc. Natl. Acad. Sci. USA 106 (2009) 169–174.

[31] C. Colussi, E. Parlanti, P. Degan, G. Aquilina, D. Barnes, P. Macpherson, P. Karran, M. Crescenzi, E. Dogliotti, M. Bignami, The mammalian mismatch repair pathway removes DNA 8-oxodGMP incorporated from the oxidized dNTP pool, Curr. Biol. 12 (2002) 912–918.

[32] M.T. Russo, M.F. Blasi, F. Chiera, P. Fortini, P. Degan, P. Macpherson, M. Furuichi, Y. Nakabeppu, P. Karran, G. Aquilina, M. Bignami, The oxidized deoxynucleoside triphosphate pool is a significant contributor to genetic instability in mismatch repair-deficient cells, Mol. Cell Biol. 24 (2004) 465–474.

[33] K. Fujikawa, H. Kamiya, H. Yakushiji, Y. Fujii, Y. Nakabeppu, H. Kasai, The oxidized forms of dATP are substrates for the human MutT homologue, the hMTH1 protein, J. Biol. Chem. 274 (1999) 18201–18205.

[34] J.P. Cai, T. Ishibashi, Y. Takagi, H. Hayakawa, M. Sekiguchi, Mouse MTH2 protein which prevents mutations caused by 8-oxoguanine nucleotides, Biochem. Biophys. Res. Commun. 305 (2003) 1073–1077.

[35] T. Ishibashi, H. Hayakawa, M. Sekiguchi, A novel mechanism for preventing mutations caused by oxidation of guanine nucleotides, EMBO Rep. 4 (2003) 479–483.

[36] M.L. Tassotto, C.K. Mathews, Assessing the metabolic function of the MutT 8-oxodeoxyguanosine triphosphatase in Escherichia coli by nucleotide pool analysis, J. Biol. Chem. 277 (2002) 15807–15812.

[37] Z.F. Pursell, J.T. McDonald, C.K. Mathews, T.A. Kunkel, Trace amounts of 8-oxo-dGTP in mitochondrial dNTP pools reduce DNA polymerase gamma replication fidelity, Nucleic Acids Res. 36 (2008) 2174–2181.

[38] S.S. Hah, J.M. Mundt, H.M. Kim, R.A. Sumbad, K.W. Turteltaub, P.T. Henderson, Measurement of 7,8-dihydro-8-oxo-2′-deoxyguanosine metabolism in MCF-7 cells at low concentrations using accelerator mass spectrometry, Proc. Natl. Acad. Sci. USA 104 (2007) 11203–11208.

[39] A. Katafuchi, A. Sassa, N. Niimi, P. Gruz, H. Fujimoto, C. Masutani, F. Hanaoka, T. Ohta, T. Nohmi, Critical amino acids in human DNA polymerases η and κ involved in erroneous incorporation of oxidized nucleotides, Nucleic Acids Res. 38 (2010) 859–867.

[40] M. Shimizu, P. Gruz, H. Kamiya, C. Masutani, Y. Xu, Y. Usui, H. Sugiyama, H. Harashima, F. Hanaoka, T. Nohmi, Efficient and erroneous incorporation of oxidized DNA precursors by human DNA polymerase η, Biochemistry 46 (2007) 5515–5522.

[41] H.J. Einolf, N. Schnetz-Boutaud, F.P. Guengerich, Steady-state and pre-steady-state kinetic analysis of 8-oxo-7,8-dihydroguanosine triphosphate incorporation and extension by replicative and repair DNA polymerases, Biochemistry 37 (1998) 13300–13312.

[42] K. Bebenek, T.A. Kunkel, Functions of DNA polymerases, Adv. Protein Chem. 69 (2004) 137–165.

[43] A. Kornberg, T.A. Baker, DNA Replication, W.H. Freeman and Co., New York, 1992, pp. 165–182.

[44] C.M. Joyce, W.S. Kelley, N.D. Grindley, Nucleotide sequence of the Escherichia coli polA gene and primary structure of DNA polymerase I, J. Biol. Chem. 257 (1982) 1958–1964.

[45] P.A. Ropp, W.C. Copeland, Cloning and characterization of the human mitochondrial DNA polymerase, DNA polymerase gamma, Genomics 36 (1996) 449–458.

[46] J.W. Hanes, D.M. Thal, K.A. Johnson, Incorporation and replication of 8-oxo-deoxyguanosine by the human mitochondrial DNA polymerase, J. Biol. Chem. 281 (2006) 36241–36248.

[47] A.A. Purmal, Y.W. Kow, S.S. Wallace, 5-Hydroxypyrimidine deoxynucleoside triphosphates are more efficiently incorporated into DNA by exonuclease-free Klenow fragment than 8-oxopurine deoxynucleoside triphosphates, Nucleic Acids Res. 22 (1994) 3930–3935.

[48] M. Yamada, T. Nunoshiba, M. Shimizu, P. Gruz, H. Kamiya, H. Harashima, T. Nohmi, Involvement of Y-family DNA polymerases in mutagenesis caused by oxidized nucleotides in Escherichia coli, J. Bacteriol. 188 (2006) 4992–4995.

[49] P. Macpherson, F. Barone, G. Maga, F. Mazzei, P. Karran, M. Bignami, 8-oxoguanine incorporation into DNA repeats in vitro and mismatch recognition by MutSα, Nucleic Acids Res. 33 (2005) 5094–5105.

[50] Y.I. Pavlov, D.T. Minnick, S. Izuta, T.A. Kunkel, DNA replication fidelity with 8-oxodeoxyguanosine triphosphate, Biochemistry 33 (1994) 4695–4701.

[51] T. Nohmi, Environmental stress and lesion-bypass DNA polymerases, Annu. Rev. Microbiol. 60 (2006) 231–253.

[52] F. Wang, W. Yang, Structural insight into translesion synthesis by DNA Pol II, Cell 139 (2009) 1279–1289.

[53] P.M. Burgers, Eukaryotic DNA polymerases in DNA replication and DNA repair, Chromosoma 107 (1998) 218–227.

[54] T. Kesti, K. Flick, S. Keranen, J.E. Syvaoja, C. Wittenberg, DNA polymerase epsilon catalytic domains are dispensable for DNA replication, DNA repair, and cell viability, Mol. Cell 3 (1999) 679–685.

[55] S. Prakash, R.E. Johnson, L. Prakash, Eukaryotic translesion synthesis DNA polymerases: specificity of structure and function, Annu. Rev. Biochem. 74 (2005) 317–353.

[56] M. de Vega, M. Salas, A highly conserved tyrosine residue of family B DNA polymerases contributes to dictate translesion synthesis past 8-oxo-7,8-dihydro-2′-deoxyguanosine, Nucleic Acids Res. 35 (2007) 5096–5107.

[57] A.S. Kamath-Loeb, A. Hizi, H. Kasai, L.A. Loeb, Incorporation of the guanosine triphosphate analogs 8-oxo-dGTP and 8-NH2-dGTP by reverse transcriptases and mammalian DNA polymerases, J. Biol. Chem. 272 (1997) 5892–5898.

[58] K. Satou, M. Hori, K. Kawai, H. Kasai, H. Harashima, H. Kamiya, Involvement of specialized DNA polymerases in mutagenesis by 8-hydroxy-dGTP in human cells, DNA Repair (Amst) 8 (2009) 637–642.

[59] M. Shimizu, P. Gruz, H. Kamiya, S.R. Kim, F.M. Pisani, C. Masutani, Y. Kanke, H. Harashima, F. Hanaoka, T. Nohmi, Erroneous incorporation of oxidized DNA precursors by Y-family DNA polymerases, EMBO Rep. 4 (2003) 269–273.

[60] S. Bailey, R.A. Wing, T.A. Steitz, The structure of T. aquaticus DNA polymerase III is distinct from eukaryotic replicative DNA polymerases, Cell 126 (2006) 893–904.

[61] M.H. Lamers, R.E. Georgescu, S.G. Lee, M. O'Donnell, J. Kuriyan, Crystal structure of the catalytic alpha subunit of E. coli replicative DNA polymerase III, Cell 126 (2006) 881–892.

[62] H. Kamiya, H. Kasai, 2-Hydroxy-dATP is incorporated opposite G by Escherichia coli DNA polymerase III resulting in high mutagenicity, Nucleic Acids Res. 28 (2000) 1640–1646.

[63] P.M. Burgers, E.V. Koonin, E. Bruford, L. Blanco, K.C. Burtis, M.F. Christman, W.C. Copeland, E.C. Friedberg, F. Hanaoka, D.C. Hinkle, C.W. Lawrence, M. Nakanishi, H. Ohmori, L. Prakash, S. Prakash, C.A. Reynaud, A. Sugino, T. Todo, Z. Wang, J.C. Weill, R. Woodgate, Eukaryotic DNA polymerases: proposal for a revised nomenclature, J. Biol. Chem. 276 (2001) 43487–43490.

[64] S. Aoufouchi, E. Flatter, A. Dahan, A. Faili, B. Bertocci, S. Storck, F. Delbos, L. Cocea, N. Gupta, J.C. Weill, C.A. Reynaud, Two novel human and mouse DNA polymerases of the polX family, Nucleic Acids Res. 28 (2000) 3684–3693.

[65] M. Garcia-Diaz, O. Dominguez, L.A. Lopez-Fernandez, L.T. de Lera, M.L. Saniger, J.F. Ruiz, M. Parraga, M.J. Garcia-Ortiz, T. Kirchhoff, J. del Mazo, A. Bernad, L. Blanco, DNA polymerase λ (Pol λ), a novel eukaryotic DNA polymerase with a potential role in meiosis, J. Mol. Biol. 301 (2000) 851–867.

[66] K. Nagasawa, K. Kitamura, A. Yasui, Y. Nimura, K. Ikeda, M. Hirai, A. Matsukage, M. Nakanishi, Identification and characterization of human DNA polymerase β 2, a DNA polymerase β-related enzyme, J. Biol. Chem. 275 (2000) 31233–31238.

[67] M. Garcia-Diaz, K. Bebenek, G. Gao, L.C. Pedersen, R.E. London, T.A. Kunkel, Structure-function studies of DNA polymerase lambda, DNA Repair (Amst) 4 (2005) 1358–1367.

[68] H. Miller, R. Prasad, S.H. Wilson, F. Johnson, A.P. Grollman, 8-oxodGTP incorporation by DNA polymerase β is modified by active-site residue Asn279, Biochemistry 39 (2000) 1029–1033.

[69] J.A. Brown, W.W. Duym, J.D. Fowler, Z. Suo, Single-turnover kinetic analysis of the mutagenic potential of 8-oxo-7,8-dihydro-2′-deoxyguanosine during gap-

filling synthesis catalyzed by human DNA polymerases λ and β, J. Mol. Biol. 367 (2007) 1258–1269.

[70] S.J. Kumar, B.J. Lamarche, M.D. Tsai, Use of damaged DNA and dNTP substrates by the error-prone DNA polymerase X from African swine fever virus, Biochemistry 46 (2007) 3814–3825.

[71] H. Ohmori, E.C. Friedberg, R.P. Fuchs, M.F. Goodman, F. Hanaoka, D. Hinkle, T.A. Kunkel, C.W. Lawrence, Z. Livneh, T. Nohmi, L. Prakash, S. Prakash, T. Todo, G.C. Walker, Z. Wang, R. Woodgate, The Y-family of DNA polymerases, Mol. Cell 8 (2001) 7–8.

[72] H. Ling, F. Boudsocq, R. Woodgate, W. Yang, Crystal structure of a Y-family DNA polymerase in action: a mechanism for error-prone and lesion-bypass replication, Cell 107 (2001) 91–102.

[73] V.G. Godoy, D.F. Jarosz, F.L. Walker, L.A. Simmons, G.C. Walker, Y-family DNA polymerases respond to DNA damage-independent inhibition of replication fork progression, EMBO J. 25 (2006) 868–879.

[74] S.J. Culp, B.P. Cho, F.F. Kadlubar, F.E. Evans, Structural and conformational analyses of 8-hydroxy-2′-deoxyguanosine, Chem. Res. Toxicol. 2 (1989) 416–422.

[75] N. Niimi, A. Sassa, A. Katafuchi, P. Gruz, H. Fujimoto, R.R. Bonala, F. Johnson, T. Ohta, T. Nohmi, The steric gate amino acid tyrosine 112 is required for efficient mismatched-primer extension by human DNA polymerase κ, Biochemistry 48 (2009) 4239–4246.

[76] A. Alt, K. Lammens, C. Chiocchini, A. Lammens, J.C. Pieck, D. Kuch, K.P. Hopfner, T. Carell, Bypass of DNA lesions generated during anticancer treatment with cisplatin by DNA polymerase η, Science 318 (2007) 967–970.

[77] R.A. Wing, S. Bailey, T.A. Steitz, Insights into the replisome from the structure of a ternary complex of the DNA polymerase III alpha-subunit, J. Mol. Biol. 382 (2008) 859–869.

[78] C.M. Joyce, T.A. Steitz, Polymerase structures and function: variations on a theme? J. Bacteriol. 177 (1995) 6321–6329.

[79] L.F. Silvian, E.A. Toth, P. Pham, M.F. Goodman, T. Ellenberger, Crystal structure of a DinB family error-prone DNA polymerase from *Sulfolobus solfataricus*, Nat. Struct. Biol. 8 (2001) 984–989.

[80] J. Trincao, R.E. Johnson, C.R. Escalante, S. Prakash, L. Prakash, A.K. Aggarwal, Structure of the catalytic core of S. cerevisiae DNA polymerase eta: implications for translesion DNA synthesis, Mol. Cell 8 (2001) 417–426.

[81] G. Maga, G. Villani, E. Crespan, U. Wimmer, E. Ferrari, B. Bertocci, U. Hubscher, 8-oxo-guanine bypass by human DNA polymerases in the presence of auxiliary proteins, Nature 447 (2007) 606–608.

[82] G. Maga, E. Crespan, U. Wimmer, B. van Loon, A. Amoroso, C. Mondello, C. Belgiovine, E. Ferrari, G. Locatelli, G. Villani, U. Hubscher, Replication protein A and proliferating cell nuclear antigen coordinate DNA polymerase selection in 8-oxo-guanine repair, Proc. Natl. Acad. Sci. USA 105 (2008) 20689–20694.

[83] B. Yeiser, E.D. Pepper, M.F. Goodman, S.E. Finkel, SOS-induced DNA polymerases enhance long-term survival and evolutionary fitness, Proc. Natl. Acad. Sci. USA 99 (2002) 8737–8741.

[84] H.J. Einolf, F.P. Guengerich, Fidelity of nucleotide insertion at 8-oxo-7,8-dihydroguanine by mammalian DNA polymerase delta. Steady-state and pre-steady-state kinetic analysis, J. Biol. Chem. 276 (2001) 3764–3771.
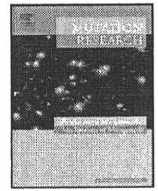
Live cell imaging of micronucleus formation and development

Manabu Yasui[a,*], Naoki Koyama[b], Tomoko Koizumi[a], Kaori Senda-Murata[c],
Yoshio Takashima[d], Makoto Hayashi[e], Kenji Sugimoto[c], Masamitsu Honma[a]

[a] Division of Genetics and Mutagenesis, National Institute of Health Sciences, 1-18-1 Kamiyoga, Setagaya, Tokyo 158-8501, Japan
[b] Graduate School of Nutrition and Environmental Sciences, University of Shizuoka, 52-1 Yada, Suruga-ku, Shizuoka 422-8526, Japan
[c] Division of Biosciences and Informatics, Osaka Prefecture University, 1-1 Gakuen-cho, Nakaku, Sakai, Osaka 599-8531, Japan
[d] Research Center for Radiation Emergency Medicine, National Institute of Radiological Sciences, 4-9-1 Anagawa, Inage, Chiba 263-8555, Japan
[e] Biosafety Research Center, Foods, Drugs and Pesticides, 582-2 Shioshinden, Iwata-shi, Shizuoka 437-1213, Japan

ARTICLE INFO

ABSTRACT

The micronucleus (MN) test is widely used to biomonitor humans exposed to clastogens and aneugens, but little is known about MN development. Here we used confocal time-lapse imaging and a fluorescent human lymphoblastoid cell line (T105GTCH), in which histone H3 and α-tubulin stained differentially, to record the emergence and behavior of micronuclei (MNi) in cells exposed to MN-inducing agents. In mitomycin C (MMC)-treated cells, MNi originated in early anaphase from lagging chromosome fragments just after chromosome segregation. In γ-ray-treated cells showing multipolar cell division, MN originated in late anaphase from lagging chromosome fragments generated by the abnormal cell division associated with supernumerary centrosomes. In vincristine(VC)-treated cells, MN formation was similar to that in MMC-treated cells, but MNi were also derived from whole chromosomes that did not align properly on the metaphase plate. Thus, the MN formation process induced by MMC, γ-rays, and VC, were strikingly different, suggesting that different mechanisms were involved. MN stability, however, was similar regardless of the treatment and unrelated to MN formation mechanisms. MNi were stable in daughter cells, and MN-harboring cells tended to die during cell cycle progression with greater frequency than cells without MN. Because of their persistence, MN may have significant impact on cells, causing genomic instability and abnormally transcribed genes.

© 2010 Elsevier B.V. All rights reserved.

1. Introduction

The micronucleus (MN) test is widely used to biomonitor humans exposed to clastogens and aneugens [1–4] and has recently become a useful tool for predicting cancer risk [5–8]. Micronuclei (MNi), which consist of chromatin (chromosomes and chromosome fragments), are formed dose-dependently in parallel with increasing concentrations of clastogens and aneugens both *in vitro* and *in vivo* [9–11].

The two basic mechanisms that give rise to MNi during M-phase are chromosome breakage and spindle apparatus defects (for review, see [12]). MNi originate as lagging acentric chromosome fragments and/or as whole chromosomes that fail to bind to the mitotic spindle during cell division. In addition, some MNi are formed from fragments induced by broken anaphase bridges [13,14]. Such mechanisms, however, are speculations based on the

analysis of fixed cells. Direct observations of the active process are few [15–17]. Moreover, the fate of MNi after they first appear at M-phase remains uncertain. If they persist in the cytoplasm during cell cycle progression [16], they might have significant impact. Genes on MN, for example, may be transcribed extrachromosomally [18–20] and influence the cell's phenotype.

Since MN formation is dynamic and rapid (lasting a few minutes) and may occur unseen behind a main nucleus, live-cell analysis at long intervals without confocal recording is inadequate to capture the event and also cannot distinguish whether a MN originates from a chromosome fragment or a whole chromosome. Here we used multi-fluorescent cells and three-dimensional, high-resolution imaging over short intervals to accurately record when, where, and how MN originates and concludes in live cells. We constructed for the study dual-color fluorescent T105GTCH cells in which histone H3 and α-tubulin were differentially expressed as fusion to monomeric Cherry (mCherry) and enhanced green fluorescent protein (EGFP), respectively. Using those cells and a high-resolution imaging system, we investigated the life cycle of MN induced by exposure to mitomycin C (MMC; a crosslinking agent), γ-rays (a strand-breaking agent), and vincristine (VC; a spindle poison).
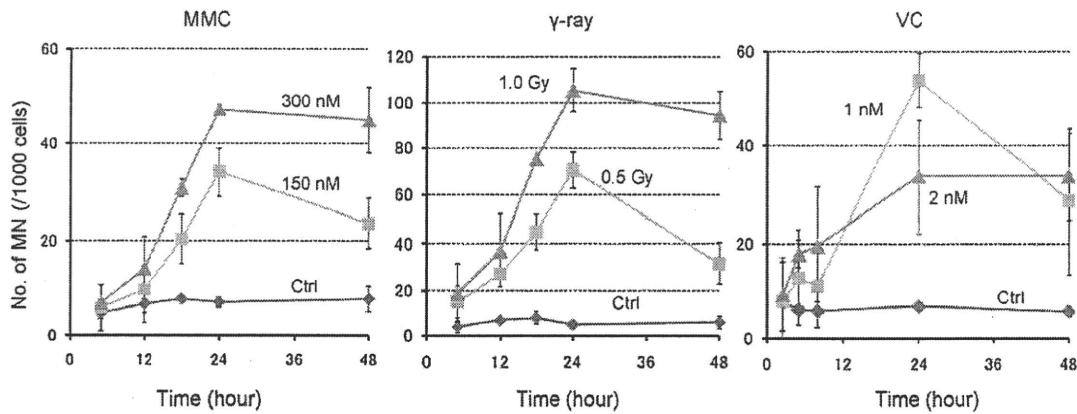
Fig. 1. *MN induction by MMC, γ-rays, and VC*: MMC, γ-rays, and VC induced MNi in T105GTCH cells dose-dependently and peaked 24 h after treatment. Control cell MN frequencies were ~5 MNi per 1000 cells.

2. Materials and methods

2.1. General

We obtained MMC from Kyowa Hakko Bio Co., Ltd. (Tokyo) and VC from Wako Pure Chemical Industries, Ltd. (Tokyo) and dissolved them in phosphate-buffered saline (Takara Bio Inc., Shiga, Japan) just before use. We delivered γ-ray irradiation with a Gammacell 40 Exactor (MDS Nordion, Canada). We purchased RPMI1640 medium, penicillin, and streptomycin from Invitrogen Corp. (USA), horse serum from JRH Biosciences (USA), sodium pyruvate from Sigma–Aldrich Corp. (USA), Dulbecco's modified Eagle's medium from Nacalai Tesque Inc. (Kyoto, Japan), and fetal calf serum from MP Biomedicals Inc. (USA).

2.2. Cell culture

We grew T105GTCH cells (derived originally from human lymphoblastoid cell line TK6 [21,22]) in RPMI1640 medium supplemented with 10% heat-inactivated horse serum, 200 μg/ml sodium pyruvate, 100 U/ml penicillin, and 100 μg/ml streptomycin and maintained them at 10^5–10^6 cells/ml at 37 °C in a 5% CO_2 atmosphere with 100% humidity. We maintained fluorescent MDA-435 cells (constructed by Sugimoto [23,24]) in Dulbecco's modified Eagle's medium containing 10–15% fetal calf serum at 37 °C in a 5% CO_2 atmosphere with 100% humidity.

2.3. Preparation of pEGFP-Tub and pmCherry-H3 plasmid

We obtained pEGFP-Tub containing human α-tubulin cDNA from BD Biosciences, Clontech. We constructed pmCherry-H3 by replacing the EGFP cDNA of pEGFP-H3 [23] with mCherry cDNA that we amplified by PCR using pRSET-B mCherry [25] (provided by Prof. Roger Y. Tsien, University of California, San Diego) as a template.

2.4. Construction of dual-color fluorescent cell line T105GTCH

pEGFP-Tub and pmCherry-H3 expression vectors, 20 μg each, were mixed with 5×10^6 TK6 cells in 100 μl Nucleofector Solution V, containing 18% Supplement 1 (Amaxa Inc., USA) and tranfected into the cells with Amaxa Nucleofector (Amaxa Inc., USA) at a setting of A-30. The vector-integrated cells were selected in the presence of G418 (750 μg/ml) and collected 10 days later. We selected single colonies of stably transfected cells with the aid of a fluorescent microscope and cultured them for 2 more weeks.

2.5. MN test

We carried out the MN test on 5×10^5 T105GTCH cells at 0, 5, 12, 18, 24, and 48 h after treatment with MMC (150 or 300 nM for 4 h followed by a PBS rinse), γ-rays (0.5 or 1 Gy), or VC (1 and 2 nM). We suspended approximately 10^6 treated cells in hypotonic KCl solution (75 mM), incubated them for 10 min at room temperature, fixed them twice with ice-cold glacial acetic acid in methanol (1:3), and resuspended them in methanol containing 1% acetic acid. We placed a drop of the suspension on a clean glass slide and allowed it to air-dry. We then stained the cells with 40 μg/ml acridine orange solution and observed them immediately with the aid of a fluorescence microscope (Olympus Corp., Tokyo). We examined at least 1000 intact interphase cells for each treatment and scored the cells containing MNi, which we defined by size as equal to or less than one-third the size of the main nucleus.

2.6. Live cell imaging for capturing MN formation

We cultured 5×10^5 T105GTCH cells in 2 ml RPMI1640 medium with a 35 mm BAM-coat dish (NOF Corp., Tokyo), which retained the cells for ~4 h on the surface, in a humid chamber set at 37 °C and 5% CO_2 on the stage of a fluorescent microscope in FV1000 system (Olympus Corp., Tokyo) equipped with

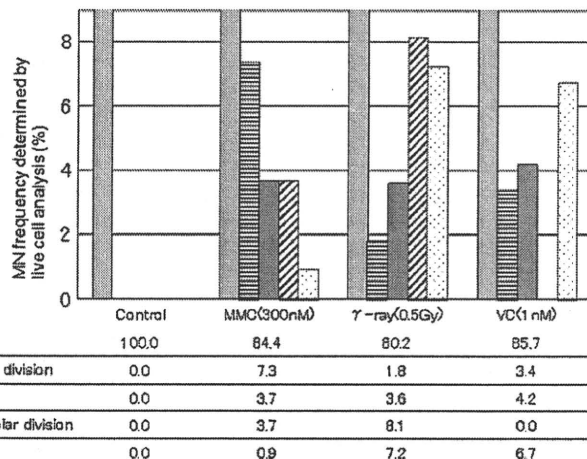|	Control	MMC(300nM)	γ−ray(0.5Gy)	VC(1 nM)
▢ Normal cell division	100.0	84.4	80.2	85.7
▤ MN formation during bipolar division	0.0	7.3	1.8	3.4
▨ Multipolar cell division	0.0	3.7	3.6	4.2
▧ MN formation during multipolar division	0.0	3.7	8.1	0.0
▢ Cell death	0.0	0.9	7.2	6.7

Fig. 2. *MN formation in T105GTCH cells analyzed by live cell imaging*: From 22 to 25 h we recorded moving images of 109 cell divisions following treatment with MMC (300 nM), 111 following irradiation with γ-rays (0.5 Gy), and 119 following treatment with VC (1 nM). MN frequencies (%) are presented by category. All control cells divided normally with no evidence of MN formation.

computer-controlled confocal and multi-stage functions. We used multi-Ar and He–Ne G lasers and 60× (1.20 NA) objective. We captured a time-lapse image every 2–3 min (z-series of 11–16 images with an interval of 1.0–2.0 μm) and reconstructed by Volocity software (Improvision Inc., USA), documenting cell division from 22 to 25 h after treatment with 300 nM MMC (109 cell divisions), 0.5 Gy γ-ray irradiation (111 cell divisions), or 1 nM VC (119 cell divisions). MN in live cell imaging was defined as a whole chromosome or chromosome fragment which is physically distinct from the main group of chromosomes. We examined at least 100 mitotic cells for each treatment and scored cell divisions that gave rise to MN, which we defined by size as equal to or less than one-third the size of the main nucleus. We distinguished between chromosomes and chromosome fragments by using criteria that a metacentric or submetacentric chromosome had two short and long arms (see Fig. 4C), but not a chromosome fragment.

2.7. Statistical analysis

MN frequencies between non-treated and treated cells were statistically analyzed by Fisher's exact test. The concentration–response relationship was evaluated by the Cochran–Armitage trend test [26].

2.8. Long-term live-cell analysis

To investigate the behavior of chromosome-originating MNi up to and through the next cell division after M-phase, we recorded the behavior of MN-bearing MDA-435 cells in which chromatin was visualized with cyan fluorescent proteins (CFP). We exposed cells to MMC (300 nM), incubated them for 24 h, and washed with PBS. We maintained the cells under minimally toxic conditions by using mild laser excitation output (~50% of the visualized control cells divided normally after 24 h) and carried out time-lapse recording at

10–20 min intervals for 24–60 h (z-series of 11–13 images with an interval of 2.0 μm).

3. Results and discussion

3.1. Toxicity of staining system

We isolated the dual-fluorescent T105GTCH clones stably showing red nuclei and green tubulin with the aid of a fluorescent microscope. The growth rate and spontaneous MN frequency for T105GTCH cells were almost the same as those reported for TK6 cells [27,28], indicating that the EGFP and mCherry fluorescent proteins were not cytotoxic.

3.2. Induced MN frequencies

Fig. 1 shows the MN frequencies induced by MMC, γ-rays, and VC over time. The spontaneous MN frequency was ~5/1000 cells (0.5%). MMC, γ-rays, and VC increased the frequencies dose-dependently, peaking at 24 h. The MN frequencies induced by 300 nM MMC, 0.5 Gy γ-ray irradiation, and 1 nM VC were similar (~5%) at 24 h, the time we started the live-cell imaging analysis. At 24 h, the growth rate of cells exposed to each of the MN-inducing agents was only ~20% lower than the growth rate of control cells.
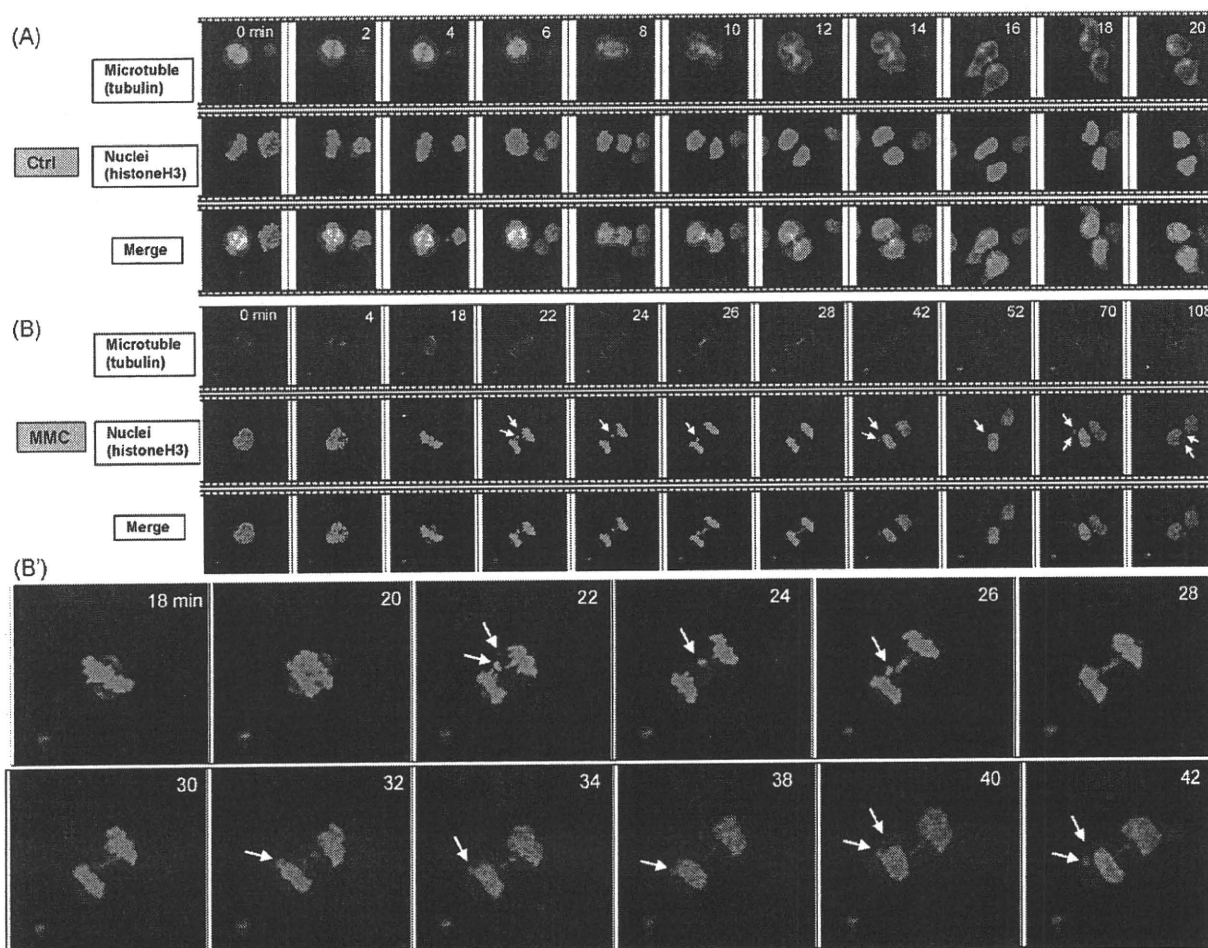

Fig. 3. Confocal live cell image analysis of cells treated with MMC, γ-rays, and VC: (A) Normal bipolar cell division (control); no MNi were observed. (B) Normal bipolar cell division in cells treated with MMC (300 nM). Chromosome fragment becoming MNi formed at 22 min, at early anaphase, and remained for 86 min (until the time-lapse recording was over). This sample corresponds to the ID number 4 in Table 1. (C) Multipolar division in cells treated with γ-rays (0.5 Gy). MNi formed at ~122 min, in late anaphase, and remained for 78 min (sample number 21 in Table 1). (D) Normal bipolar division in cells treated with VC (1 nM). MN formed at 22 min, at early anaphase, and repeatedly attached to a daughter nucleus and detached from it (sample number 24 in Table 1).
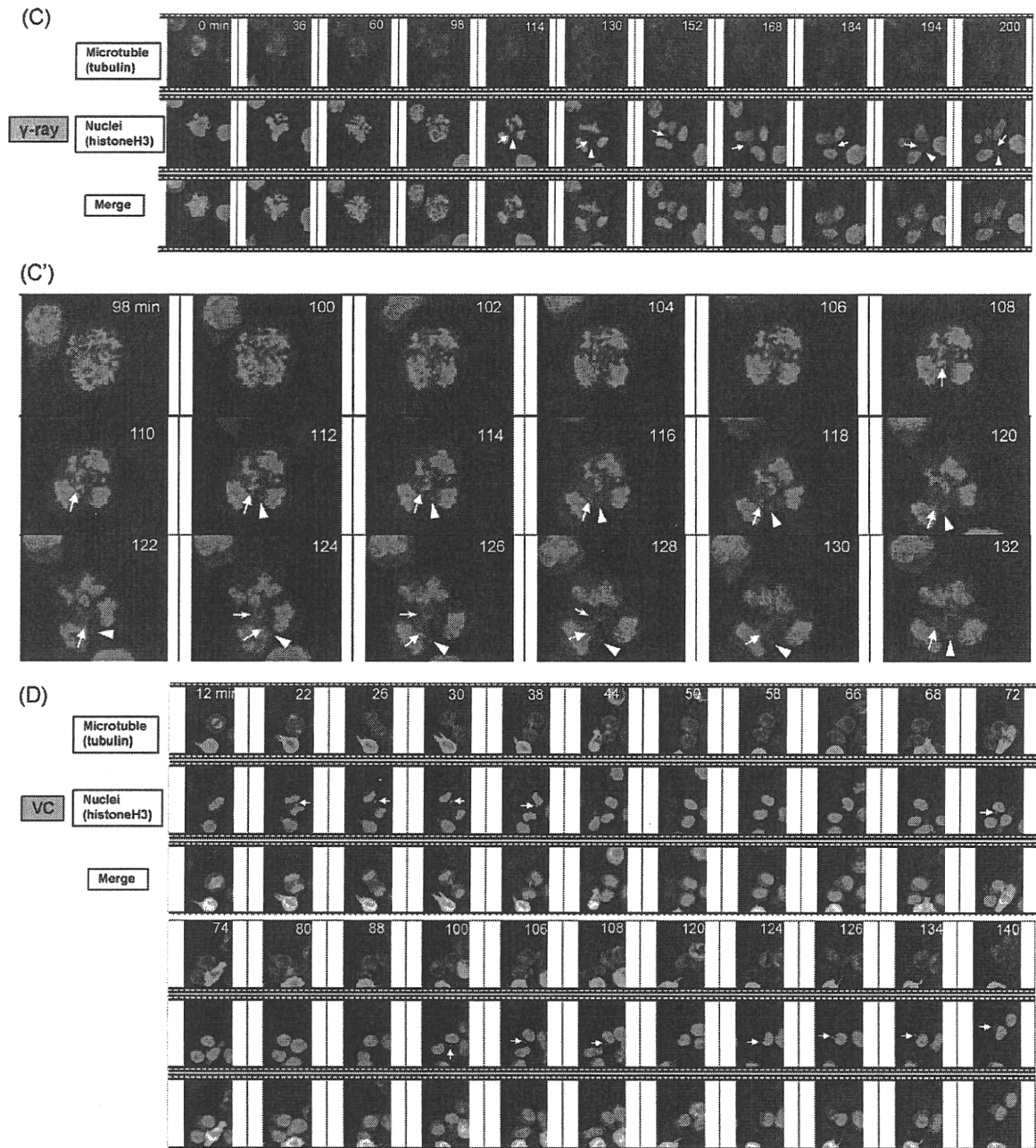
Fig. 3. (Continued)

Following exposure to 1 nM VC, ~50% of cells passed the mitotic checkpoint and were used in the live-cell analysis.

3.3. MN emergence captured by confocal time-lapse microscopy

We found at least one MN during bipolar or multipolar mitosis in 12 (~11%) MMC-treated cells, 11 (~10%) γ-ray irradiated cells, and 4 (~3%) VC-treated cells. Fig. 2 shows the categories of cell division that led to MN formation and mitotic catastrophe. Mitotic catastrophe was defined as cell death during M-phase (from prophase to telophase). All MN originated from lagging chromosomes or chromatid fragments and whole chromosomes in this study.

Confocal time-lapse microscopy of control cells recorded normal division with no MN formation evident (Figs. 2 and 3A). Fig. 3B shows the time course of typical MN formation in MMC-treated

cells. The MNi originated from two lagging chromosome fragments just after chromosome segregation at early anaphase and immediately became spherical, resulting in the formation of small and large MNi of appropriate thickness for the size of the fragment (arrows in Fig. 3B and B′). Subsequently, the MNi collided with the main nucleus, disappeared from the view (26–30 min), and came out from it at 32 min as shown in Fig. 3B′. The two MNi sometimes came into contact but were independent and did not condense into a single MN by the end of the time-lapse recording (108 min).

Following γ-ray irradiation, multipolar division occurred with high-frequency (11.7%), and 70% of the daughter cells formed MN during divisions that involved 3 or 4 spindle poles (Figs. 2 and 3C). Our finding that γ-ray irradiation increases the abnormal replication of supernumerary centrosomes is in agreement with a report by Sato and colleagues [29]. MN induction involving multipo-
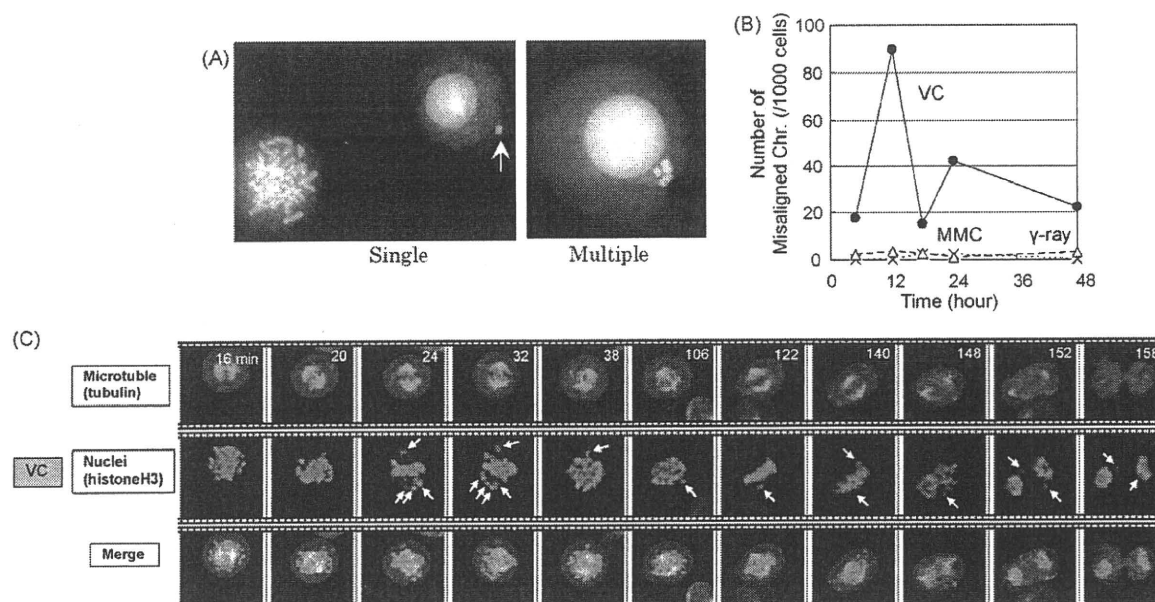
Fig. 4. *Metaphase misalignment in VC-treated cells*: (A) VC-treated cells showing misaligned chromosome, single (left panel) and multiple (right panel), in MN test. (B) The frequency of misaligned chromosomes peaked at 12 h in only VC-treated cells. (C) Misaligned chromosomes were captured at 6–9 h after VC treatment and promoted MN formation and aneuploid. Metacentric and submetacentric chromosomes had two short and long arms and were structurally different from a chromosome fragment.

lar mitosis originated mainly from broken chromosomes at late anaphase, and the MNi were not spherical, showing that MNi induced by γ-rays formed differently from those induced by MMC. In normal cell division, the two sets of chromatid were pulled toward two spindle poles for equal distribution into daughter cells (Fig. 3A) [30]. In multipolar mitosis, however, chromosomes were pulled toward to 3 or 4 sides of the multipolar spindle and simultaneously broken off into small pieces (100–108 min) at early anaphase, resulting in the formation of broken chromosome specks (arrows in Fig. 3C'). We here define that a chromosome speck is generated by fatal breakage of chromosome or chromosome fragment in anaphase and is not spherical. Fragments and specks mostly entered the main nucleus (108–118 min) but some specks did not re-enter the main nucleus. At the beginning of telophase, the more lagging fragments (Fig. 3C and C', arrowheads) also could not enter the main nucleus in daughter cells. Meanwhile, a fraction of lagging specks disappeared in mid-body when the cells split at telophase (124–128 min), indicating DNA loss (Fig. 3C', yellow arrows).

Following VC treatment, spherical MNi (3.4%) formed at anaphase similar to the way they formed following MMC treatment (Fig. 3B and D). Cell death (6.7%) by mitotic catastrophe also occurred due to detrimental karyotypic changes induced by VC. Another factor causing the MN frequency to increase was intact chromosomes that did not align on the metaphase plate (Fig. 4C, arrows), which were also detectable in the MN test (Fig. 4A). The frequency of misaligned chromosomes peaked at 12 h (Fig. 4B). We captured some misaligned chromosomes becoming MNi, but the frequency was low because of a p53-dependent check point [30,31] in the T105GTCH cells during meta-anaphase (Fig. 4C). Thus, the initiation time for MN formation induced by VC began at metaphase.

3.4. MN formation mechanisms varied with the MN-inducing agent

The spherical MN had an appropriate thickness for the size of the whole chromosome (Fig. 4C) and chromosome fragment (Fig. 3B and D). It was induced by MMC and VC treatment in this study. The aspherical MN originated from chromosome specks generated by fatal breakage of chromosome or chromosome fragment induced

by γ-rays in this paper. The density (DNA content) of aspherical MN would be lower than that of spherical one because the chromosome specks were formed by the complex fragmentation and expansion of small chromosome fragments which pulled toward to 3 or 4 sides of multipolar spindle during cell division, resulting in the formation of low density MN (Fig. 3C).

MMC, a potent DNA crosslinking agent [32], induces fragmented chromosomes. We found that the frequency of MN originating from lagging chromosome fragments at anaphase during normal mitosis was induced by the 3 agents in the order MMC > VC > γ-rays (Fig. 2). Following VC treatment, and only VC treatment (Fig. 4B), we observed MNi formed by intact chromosomes that did not align at the metaphase plate, but we did not detect any during multipolar cell division (Fig. 2). That is because VC binds to tubulin dimers, inhibiting assembly of microtubule structures, but it is not a DNA damaging agent (VC is Ames-test negative) and so does not promote chromosome fragments. In multipolar division, in contrast, γ-rays induced more MNi than MMC (Fig. 2). That can be explained by the fact that γ-rays can simultaneously induce DNA strand breaks (forming chromosome fragments) and abnormal amplification of centrosomes (increasing the frequency of aberrant mitoses and chromosome segregation errors). Thus, the typical events of MN formation induced by MMC, γ-rays, and VC were strikingly different, suggesting that different mechanisms were involved.

3.5. Behavior and stability of MNi after cell division

MNi first appeared during M-phase, and we tracked them and studied their behavior and stability during G1-phase with T105GTCH cells. The MNi were dynamic and sometimes moved behind the nucleus, and they remained stable in the cytoplasm of daughter cells for a few hours (until the time-lapse recording was over) as shown by the column of Stability of MN in Table 1. That observation was consistent with a previous report using the UPCI SCC oral squamous cell carcinoma cell line [16]. We also found that MN stability was similar and unrelated to the toxic action of MN-inducing MMC, γ-rays, and VC (Table 1). Interestingly, only in bipolar mitoses, MNi repeatedly attached to a daughter nucleus and detached from it at a later time (Fig. 3D, corresponding to the

Table 1
MN formation and stability observed in T105GTCH cells following treatment with MN-inducing agents.

MN-inducing agent	Sample ID number	Number of mitotic spindles	Time of MN formation (min)	Time when MNi interacted with main nucleus (min)[a]	Stability of MN (min)
MMC	1	2	14	22-**26**-28	–
	2	2	14	16-**24**-26-**30**-34	–
	3	2	6	20-22-38-**44**	–
	4	2	22	28-**32**	–
	5	2	20	42	22
	6	2	10	20	10
	7	2	12	54	42
	8	2	16	34	18
	9	3	6	–	16
	10	3	6	–	20
	11	4	28	–	20
	12	3	6	–	50
γ-Rays	13	2	20	62	42
	14	2	90	168	78
	15	4	48	116	68
	16	3	40	–	20
	17	3	36	–	24
	18	3	22	–	40
	19	3	90	–	40
	20	3	20	–	42
	21	4	122	–	78
	22	4	30	–	140
	23	4	48	–	250
VC	24	2	22	38-**72**-74-**92**-118-**124**	–
	25	2	156	182	26
	26	2	68	96	28
	27	2	40	–	110

[a] Italic and bold types indicate when MN attached to and detached from the main nucleus, respectively.

sample number 24 in Table 1). The relationship between MN interaction with the main nucleus and the polar number in cell division, however, is unclear.

In long-term live-cell analysis performed by under mild laser excitation output, approximately 50% of non-treated MDA-435 control cells normally divided after 24 h (Animation 1). Animation 2 shows typical MN fates in MMC-treated MDA-435 cells we observed with long-term live-cell analysis. As shown in Fig. 5, only 5 (5%) of the 98 interphase cells harboring MMC-induced MNi proceeded to M-phase (Fig. 5c), and 4 cells of them underwent mitotic catastrophe (d). MNi in 68 (69%) of the cells persisted in the cytoplasm for the full observation time (a). Thus, MN stability was similar to that obtained from the above experiment with T105GTCH cells. Besides, cell cycle progression was delayed in MN-

harboring cells, and their cell death was approximately 2.5-fold higher than that of cells without MN because of their genomic instability increased by MN and the laser excitation effect (b). It is possible that all MN-bearing cells eventually die (Fig. 5(b) and (d)). Thus, MN may have significant impact on cells because of their persistence. MN in 1 (1%) of the cells disappeared from the cytoplasm, where it may have been degraded. We also observed blebbing MNi in 2% of the cells. In a previous report [33], an elimination mechanism of MN from the cell was suggested, but we did not observe that in this study.

In conclusion, in this confocal microscopic study of live T105GTCH cells exposed to three kinds of MN-inducing agents, we found that MNi can be generated by strikingly different mechanisms. After MNi emerge, however, their stabilities are similar and unrelated to MN formation mechanisms. Long-term live-cell analysis of chromatin-visualized MDA-435 cells suggested that MN-harboring cells tended to die during cell cycle progression with greater frequency than cells without MN. Because of their persistence, MN may have significant impact on cells, causing genomic instability and abnormally transcribed genes.

Conflict of interest statement

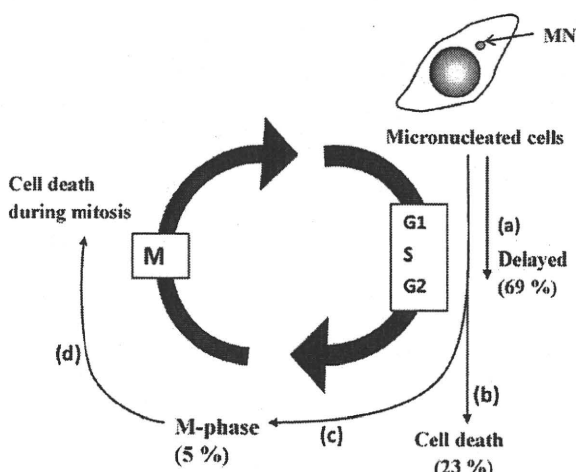The authors declare that there are no conflicts of interest.

Fig. 5. Diagram of fates of micronucleated cells based on long-term live-cell imaging of fluorescent MDA-435 cells exposed to MMC (300 nM).

Appendix A. Supplementary data

Supplementary data associated with this article can be found, in the online version, at doi:10.1016/j.mrfmmm.2010.07.009.

References

[1] H. Weng, K. Morimoto, Differential responses to mutagens among human lymphocyte subpopulations, Mutat. Res. 672 (2009) 1–9.
[2] N. Holland, C. Bolognesi, M. Kirsch-Volders, S. Bonassi, E. Zeiger, S. Knasmueller, M. Fenech, The micronucleus assay in human buccal cells as a tool for biomonitoring DNA damage: the HUMN project perspective on current status and knowledge gaps, Mutat. Res. 659 (2008) 93–108.
[3] R. Mateuca, N. Lombaert, P.V. Aka, I. Decordier, M. Kirsch-Volders, Chromosomal changes: induction, detection methods and applicability in human biomonitoring, Biochimie 88 (2006) 1515–1531.
[4] M. Fenech, The in vitro micronucleus technique, Mutat. Res. 455 (2000) 81–95.
[5] R.A. El Zein, M.B. Schabath, C.J. Etzel, M.S. Lopez, J.D. Franklin, M.R. Spitz, Cytokinesis-blocked micronucleus assay as a novel biomarker for lung cancer risk, Cancer Res. 66 (2006) 6449–6456.
[6] S. Bonassi, A. Znaor, M. Ceppi, C. Lando, W.P. Chang, N. Holland, M. Kirsch-Volders, E. Zeiger, S. Ban, R. Barale, M.P. Bigatti, C. Bolognesi, A. Cebulska-Wasilewska, E. Fabianova, A. Fucic, L. Hagmar, G. Joksic, A. Martelli, L. Migliore, E. Mirkova, M.R. Scarfi, A. Zijno, H. Norppa, M. Fenech, An increased micronucleus frequency in peripheral blood lymphocytes predicts the risk of cancer in humans, Carcinogenesis 28 (2007) 625–631.
[7] A.K. Nersesyan, Possible role of the micronucleus assay in diagnostics and secondary prevention of cervix cancer: a minireview, Tsitol. Genet. 41 (2007) 64–66.
[8] D. Varga, W. Vogel, A. Bender, H. Surowy, C. Maier, R. Kreienberg, H. Deissler, G. Sauer, Increased radiosensitivity as an indicator of genes conferring breast cancer susceptibility, Strahlenther. Onkol. 183 (2007) 655–660.
[9] H.J. Evans, G.J. Neary, F.S. Williamson, The relative biological efficiency of single doses of fast neutrons and gamma-rays on Vicia faba roots and the effect of oxygen. Part II. Chromosone damage: the production of micronuclei, Int. J. Radiat. Biol. 1 (1959) 216–229.
[10] J.A. Heddle, A.V. Carrano, The DNA content of micronuclei induced in mouse bone marrow by gamma-irradiation: evidence that micronuclei arise from acentric chromosomal fragments, Mutat. Res. 44 (1977) 63–69.
[11] M. Hayashi, T. Sofuni, M. Ishidate Jr., Kinetics of micronucleus formation in relation to chromosomal aberrations in mouse bone marrow, Mutat. Res. 127 (1984) 129–137.
[12] H. Norppa, G.C. Falck, What do human micronuclei contain? Mutagenesis 18 (2003) 221–233.
[13] W.S. Saunders, M. Shuster, X. Huang, B. Gharaibeh, A.H. Enyenihi, I. Petersen, S.M. Gollin, Chromosomal instability and cytoskeletal defects in oral cancer cells, Proc. Natl. Acad. Sci. U.S.A. 97 (2000) 303–308.
[14] P. Thomas, K. Umegaki, M. Fenech, Nucleoplasmic bridges are a sensitive measure of chromosome rearrangement in the cytokinesis-block micronucleus assay, Mutagenesis 18 (2003) 187–194.
[15] X. Rao, Y. Zhang, Q. Yi, H. Hou, B. Xu, L. Chu, Y. Huang, W. Zhang, M. Fenech, Q. Shi, Multiple origins of spontaneously arising micronuclei in HeLa cells: direct evidence from long-term live cell imaging, Mutat. Res. 646 (2008) 41–49.

[16] D.R. Hoffelder, L. Luo, N.A. Burke, S.C. Watkins, S.M. Gollin, W.S. Saunders, Resolution of anaphase bridges in cancer cells, Chromosoma 112 (2004) 389–397.
[17] W. Rens, L. Torosantucci, F. Degrassi, M.A. Ferguson-Smith, Incomplete sister chromatid separation of long chromosome arms, Chromosoma 115 (2006) 481–490.
[18] K. Utani, J.K. Kawamoto, N. Shimizu, Micronuclei bearing acentric extrachromosomal chromatin are transcriptionally competent and may perturb the cancer cell phenotype, Mol. Cancer Res. 5 (2007) 695–704.
[19] B. Labidi, M. Gregoire, S. Frackowiak, D. Hernandez-Verdun, M. Bouteille, RNA polymerase activity in PtK1 micronuclei containing individual chromosomes. An in vitro and in situ study, Exp. Cell Res. 169 (1987) 233–244.
[20] H. Kato, A.A. Sandberg, Chromosome pulverization in human cells with micronuclei, J. Natl. Cancer Inst. 40 (1968) 165–179.
[21] M. Honma, M. Hayashi, T. Sofuni, Cytotoxic and mutagenic responses to X-rays and chemical mutagens in normal and p53-mutated human lymphoblastoid cells, Mutat. Res. 374 (1997) 89–98.
[22] M. Honma, M. Sakuraba, T. Koizumi, Y. Takashima, H. Sakamoto, M. Hayashi, Non-homologous end-joining for repairing I-SceI-induced DNA double strand breaks in human cells, DNA Repair (Amst) 6 (2007) 781–788.
[23] K. Sugimoto, T. Urano, H. Zushi, K. Inoue, H. Tasaka, M. Tachibana, M. Dotsu, Molecular dynamics of Aurora-A kinase in living mitotic cells simultaneously visualized with histone H3 and nuclear membrane protein importinalpha, Cell Struct. Funct. 27 (2002) 457–467.
[24] K. Sugimoto, K. Senda-Murata, S. Oka, Construction of three quadruple-fluorescent MDA435 cell lines that enable monitoring of the whole chromosome segregation process in the living state, Mutat. Res. 657 (2008) 56–62.
[25] B.A. Kruskal, C.H. Keith, F.R. Maxfield, Thyrotropin-releasing hormone-induced changes in intracellular [Ca2+] measured by microspectrofluorometry on individual quin2-loaded cells, J. Cell Biol. 99 (1984) 1167–1172.
[26] T. Matsushima, M. Hayashi, A. Matsuoka, M. Ishidate Jr., K.F. Miura, H. Shimizu, Y. Suzuki, K. Morimoto, H. Ogura, K. Mure, K. Koshi, T. Sofuni, Validation study of the in vitro micronucleus test in a Chinese hamster lung cell line (CHL/IU), Mutagenesis 14 (1999) 569–580.
[27] Y. Luan, T. Suzuki, R. Palanisamy, Y. Takashima, H. Sakamoto, M. Sakuraba, T. Koizumi, M. Saito, H. Matsufuji, K. Yamagata, T. Yamaguchi, M. Hayashi, M. Honma, Potassium bromate treatment predominantly causes large deletions, but not GC > TA transversion in human cells, Mutat. Res. 619 (2007) 113–123.
[28] N. Honma, M. Sakuraba, M. Sakuraba, T. Koizumi, Y. Takashima, M. Hayashi, H. Matsufuji, K. Yamagata, S. Masuda, N. Kinae, M. Honma, Genotoxicity of acrylamide and glycidamide in human lymphoblastoid TK6 cells, Mutat. Res. 603 (2006) 151–158.
[29] N. Sato, K. Mizumoto, M. Nakamura, H. Ueno, Y.A. Minamishima, J.L. Farber, M. Tanaka, A possible role for centrosome overduplication in radiation-induced cell death, Oncogene 19 (2000) 5281–5290.
[30] K. Fukasawa, Centrosome amplification, chromosome instability and cancer development, Cancer Lett. 230 (2005) 6–19.
[31] Y Uetake, G. Sluder, Cell cycle progression after cleavage failure: mammalian somatic cells do not possess a "tetraploidy checkpoint", J. Cell Biol. 165 (2004) 609–615.
[32] M. Tomasz, Mitomycin C: small, fast and deadly (but very selective), Chem. Biol. 2 (1995) 575–579.
[33] J.H. Ford, C.J. Schultz, A.T. Correll, Chromosome elimination in micronuclei: a common cause of hypoploidy, Am. J. Hum. Genet. 43 (1988) 733–740.

Research Article

Genotoxicity of Acrylamide In Vitro: Acrylamide Is Not Metabolically Activated in Standard In Vitro Systems

Naoki Koyama,[1,2] Manabu Yasui,[1] Yoshimitsu Oda,[3] Satoshi Suzuki,[4]
Tetsuo Satoh,[4] Takuya Suzuki,[5] Tomonari Matsuda,[5] Shuichi Masuda,[2]
Naohide Kinae,[2] and Masamitsu Honma[1]*

[1]Division of Genetics and Mutagenesis, National Institute of Health Sciences,
1-18-1 Kamiyoga, Setagaya-ku, Tokyo, Japan
[2]Laboratory of Food Hygiene, Graduate School of Food and Nutritional
Sciences, University of Shizuoka, 52-1 Yada, Shizuoka-shi, Shizuoka, Japan
[3]Department of Applied Chemistry, Faculty of Science Engineering, Kinki
University, 3-4-1, Kowakae, Higashiosaka-shi, Japan
[4]HAB Research Institute, Cornea Center Building, Ichikawa General Hospital,
5-11-13 Sugano, Ichikawa, Chiba, Japan
[5]Research Center for Environmental Quality Management, Kyoto University, 1-2
Yumihama, Otsu, Shiga, Japan

The recent finding that acrylamide (AA), a genotoxic rodent carcinogen, is formed during the frying or baking of a variety of foods raises human health concerns. AA is known to be metabolized by cytochrome P450 2E1 (CYP2E1) to glycidamide (GA), which is responsible for AA's in vivo genotoxicity and probable carcinogenicity. In in-vitro mammalian cell tests, however, AA genotoxicity is not enhanced by rat liver S9 or a human liver microsomal fraction. In an attempt to demonstrate the in vitro expression of AA genotoxicity, we employed Salmonella strains and human cell lines that overexpress human CYP2E1. In the umu test, however, AA was not genotoxic in the CYP2E1-expressing Salmonella strain or its parental strain. Moreover, a transgenic human lymphoblastoid cell line overexpressing CYP2E1 (h2E1v2) and its parental cell line (AHH-1) both showed equally weak cytotoxic and genotoxic responses to high (>1 mM) AA concentrations. The DNA adduct N7-GA-Gua, which is detected in liver following AA treatment in vivo, was not substantially formed in the in vitro system. These results indicate that AA was not metabolically activated to GA in vitro. Thus, AA is not relevantly genotoxic in vitro, although its in vivo genotoxicity was clearly demonstrated. Environ. Mol. Mutagen. 52:12–19, 2011. © 2010 Wiley-Liss, Inc.

Key words: acrylamide; glycydamide; cytochrome P450 2E1 (CYP2E1); in vitro tests; Salmonella

INTRODUCTION

Recently, low levels of acrylamide (AA), a synthetic chemical widely used in industry, were detected in a variety of cooked foods [Tareke et al., 2000; Mottram et al., 2002]. It has been proposed that AA forms during frying and baking principally by the Maillard reaction between asparagine residues and glucose [Stadler et al., 2002; Tornqvist, 2005]. This finding raised concerns about a health risk for the general population [Tareke et al., 2002; Rice, 2005].

The International Agency for Research on Cancer classifies AA as 2A, a probable human carcinogen [IARC, 1994]. Because AA clearly induces gene mutations and micronuclei in mice, it could be a genotoxic carcinogen [Cao et al., 1993; Abramsson-Zetterberg, 2003; Manjanatha et al., 2005]. AA is metabolized by cytochrome

P450 2E1 (CYP2E1) to glycidamide (GA), which can react with cellular DNA and protein [Sumner et al., 1999; Ghanayem et al., 2005a; Rice, 2005]. Two major

Environmental and Molecular Mutagenesis. DOI 10.1002/em

Genotoxicity of Acrylamide In Vitro   13

GA-DNA adducts, N7-(2-carbamoyl-2-hydroxyethyl)-gua-nine (N7-GA-Gua) and N3-(2-carbamoyl-2-hydroxyethyl)-adenine (N3-GA-Ade), have been identified in mice and rats treated with AA or GA [Segerback et al., 1995; Gamboa da Costa et al., 2003; Doerge et al., 2005], with the level of N7-GA-Gua being 100 times as high as the level of N3-GA-Ade in the test organ [Gamboa da Costa et al., 2003]. It is likely that these DNA adducts are responsible for AA's in vivo genotoxicity [Carere, 2006; Ghanayem and Hoffler, 2007]. In our previous study, however, AA did not induce micronuclei in human lymphoblastoid TK6 cells in the presence of rat liver S9, although the genotoxicity of N-di-N-butylnitrosamine (DBN), which is also metabolized by CYP2E1, was enhanced under the same conditions [Koyama et al., 2006]. Other in vitro genotoxicity studies have also failed to demonstrate the metabolic activation of AA in the presence of S9 [Knaap et al., 1988; Tsuda et al., 1993; Dearfield et al., 1995; Friedman, 2003]. It may be because most S9 preparations have low CYP2E1 activity [Calleman et al., 1990; Hargreaves et al., 1994].

In an attempt to demonstrate the genotoxicity of AA in vitro, we tested the compound using bacteria and mammalian cell lines that express CYP2E1. S. typhimurium OY1002/2E1 strain expresses respective human CYP2E1 enzyme and NADPH-cytochrome P450 reductase (reductase), and bacterial O-acetyltransferase [Oda et al., 2001]. Using the strain, as well as its parental strain not expressing these enzymes, we conducted an umu assay to evaluate induction of cytotoxicity and DNA damage by AA relative to that induced by its metabolite GA. The principle of the umu assay is based on the ability of the DNA-damaging agents inducing the umu operon. Monitoring the levels of umu operon expression enables us to quantitatively detect environmental mutagens [Oda et al., 1985]. In addition, we evaluated the relative mutagenicity of AA vs. GA in assays using transgenic human lymphoblastoid cell lines. Induction of gene mutation at the TK locus and of chromosome damage leading to micronucleus (MN) formation were assessed in the h2E1v2 which overexpress human CYP2E1 [Crespi et al., 1993a], vs. its parental cell line, AHH-1. We also investigated the relationship between AA genotoxicity and the formation N7-GA-Gua (derived from GA) in the in vitro mammalian cell system.

MATERIALS AND METHODS

Bacterial Strains, Cell Lines, Chemicals, and Human Liver Microsomal Fraction

For the bacterial tests, we used umu strain S. typhimurium OY1002/2E1, which expresses human CYP2E1, reductase, and bacterial O-acetyltransferase, and its parental strain, S. typhimurium TA1535/pSK1002 that does not express these enzymes [Oda et al., 2001].

For the mammalian cell tests, we used human lymphoblastoid cell lines, TK6, AHH-1, and h2E1v2. The TK6 cell line has been described previously [Honma et al., 1997]. The AHH-1 and h2E1v2 cell lines were kindly gifted from Dr. Charles Crespi (BD Bio Sciences, Bedford, MA).

AHH-1 is a clonal isolate, derived from RPMI 1788 cells, which was selected for sensitivity to benzo[a]pyrene [Crespi and Thilly, 1984]. AHH-1 shows high activity of endogenous CYP1A1. Heterozygosity of AHH-1 cells at thymidine kinase (TK) locus was derived in a two-step selection process utilizing the frameshift mutagen, ICR-191. The AHH-1 cell line was then transfected with plasmids encoding human CYP2E1 enzymes, generating h2E1v2 cell line. AHH-1 expresses CYP1A1 and h2E1v2 expresses both CYP1A1 and CYP2E1 [Crespi et al., 1993a,b].

We purchased AA (CAS No. 79-06-1) and GA (CAS No. 5694-00-8) from Wako Pure Chemical (Tokyo) and dissolved them in phosphate-buffered saline just before use. We purchased N-di-N-methylnitorosamine (DMN) (CAS No. 62-75-9) from Sigma Aldrich Japan (Tokyo) and dissolved it in DMSO as a positive control for use. We purchased liver S9 prepared from SD rats treated with phenobarbital and 5,6-benzoflavone from the Oriental Yeast (Tokyo). The human liver S9 (HLS-104) was prepared from a human liver sample, which was legally procured from the NDRI (National Disease Research Interchange) in Philadelphia, USA, with permission to use for research purpose only. HLS-104 showed high activity of CYP2E1 [Hakura et al., 2005]. We prepared microsomal fraction from the S9 according to an established procedure [Suzuki et al., 2000]. We prepared the S9- or microsome-mix by mixing 4 ml S9 or microsomal fraction with 2 ml each of 180 mg/ml glucose-6-phosphate, 25 mg/ml NADP, and 150 mM KCl. CYP2E1 activity of the S9 and microsomal fractions were determined as the activity of chlorzaxazone 6-hydroxylation according to the method of Ikeda et al. [2001].

We grew the cell lines in RPMI1640 medium (Gibco-BRL, Life Technology, Grand Island, NY) supplemented with 10% heat-inactivated horse serum (JRH Biosciences, Lenexa, KS), 200 µg/ml sodium pyruvate, 100 U/ml penicillin, and 100 µg/ml streptomycin, and we maintained the cultures at 10^5-10^6 cells/ml at 37°C in a 5% CO_2 atmosphere with 100% humidity.

umu Assay

The umu assay was carried out by the method of Aryal et al. [1999, 2000] with slight modification. Overnight cultures of tester strains were diluted 100-fold with TGlyT medium (1% Bactotryptone, 0.5% NaCl (w/v), 0.2% glycerol (v/v), and 1 µg of tetracycline/ml, 1.0 mM IPTG, 0.5 mMδ-ALA, and 250 ml of trace element mixture/l) [Sandhu et al., 1994]. The culture was incubated for 1 hr at 37°C and then 0.75 ml aliquots of TGA culture (OD$_{600}$: 0.25–0.3) and human. Induction of the umuC gene by HCAs in different strains was determined by measuring cellular β-galactosidase activity, as described by Oda et al. [1985]. Cell toxicity was determined in reaction mixture by measuring the optical density change at 600 nm.

Mammalian Cell Assays Measuring Gene Mutation and Chromosome Damage

We incubated 20-ml aliquots of TK6, AHH-1, or h2E1v2 cell suspensions (5.0×10^5 cells/ml) treated with serially diluted AA, GA, or DMN in the presence or absence of S9 or microsomes at 37°C for 4 hr, washed them once, resuspended them in fresh medium, and cultured them in new flasks for the MN and TK assays. For TK6 cells, we also seeded cells into the 96-well plates (1.6 cells/well) to determine plating efficiency (PE0).

Forty-eight hours after treating the cells, we prepared the MN test samples as previously reported [Koyama et al., 2006]. At least, 1,000 intact interphase cells for each treatment were examined, and the cells containing MN were scored. The MN frequencies between nontreated and treated cells were statistically analyzed by Fisher's exact test. The concentration–response relationship was evaluated by the Cochran-Armitage trend test [Matsushima et al., 1999].

We maintained the cultures another 24 hr to allow phenotypic expression prior to plating for determination of the mutant fractions. After the expression time, to isolate the TK deficient mutants, we seeded the cells into 96-well plates in the presence of 3.0 µg/ml trifluorothymidine (TFT).
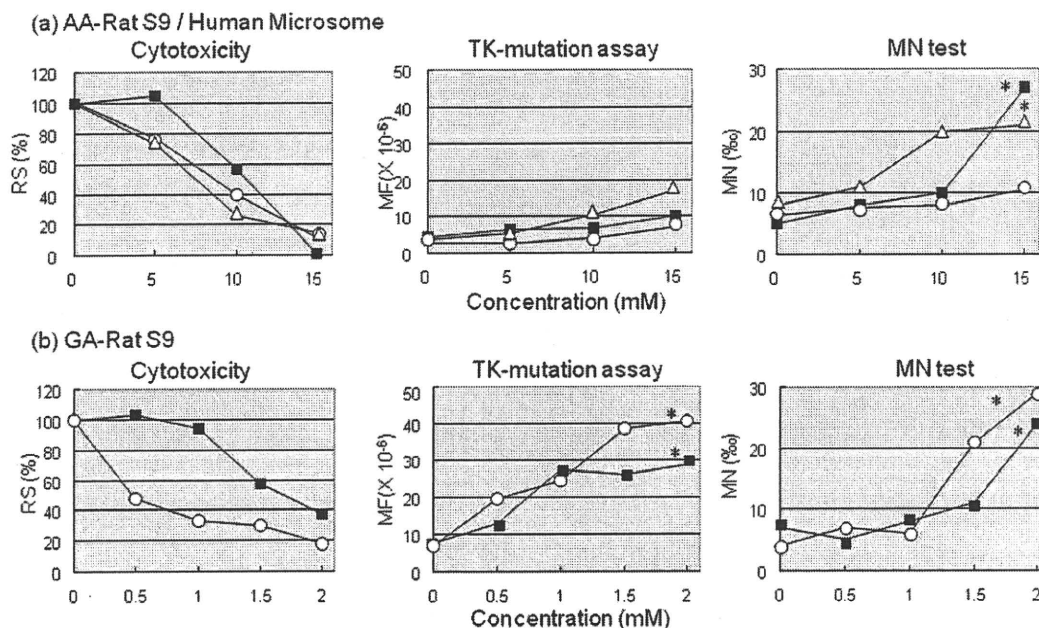
Fig. 1. Cytotoxic (relative survival, RS) and genotoxic (TK and MN assays) responses of TK6 cells treated with AA or GA for 4 hr with or without metabolic activation. (a) TK6 cells were treated with AA without (■) or with (○) rat liver S9 or human microsomes (△). (b) TK6 cells were treated with GA without (■) or with (○) rat liver S9. *$P < 0.05$ (Omori method for TK-mutation assay, trend test for MN assay).

We also seeded cells into the 96-well plates in the absence of TFT to determine plating efficiency (PE3). TK6 cells were seeded at 40,000 cells/well and 1.6 cell/well for TFT and PE plates, respectively. AHH-1 and h2E1v2 cells were seeded at 5,000 cells/well and 3.2 cells/well for TFT and PE plates, respectively. All plates were incubated at 37°C in 5% CO_2 in a humidified incubator. We scored for the colonies in the PE plates at 14th day after plating, and scored for the colonies in the TFT plate on the 28th day after plating. Mutation frequencies were calculated according to the Poisson distribution [Furth et al., 1981]. The data were statistically analyzed by Omori's method, which consists of a modified Dunnett's procedure for identifying clear negative, a Simpson-Margolin procedure for detecting downturn data, and a trend test to evaluate the dose-dependency [Omori et al., 2002]. We evaluated cytotoxicity for TK6 by relative survival (RS), which is calculated from plating efficiency (PE0), and for AHH-1 and h2E1v2 by relative suspension growth (RSG), which is calculated from cell growth rate during 3 days expression period.

Western Blot Analysis

A goat polyclonal anti-rat CYP2E1 antibody (Daiichi Pure Chemical, Tokyo) and rabbit anti-rat actin (Sigma, St. Louis, MO) were used as primary antibodies. AP-conjugated secondary antibody (Cappel, Organon Technika Corp., West Chester, PA) was used to detect primary antibody signals.

DNA Adduct Assay

As a standard for LC/MS/MS analysis, N7-GA-Gua and [$^{15}N_5$]-labeled N7-GA-Gua were synthesized as described previously [Gamboa da Costa et al., 2003]. DNA was extracted from the cells by using DNeasy 96 Blood &Tissue Kit (QIAGEN, Düsseldorf) and incubated at 37°C for 48 hr for deprination. An aliquot of the [$^{15}N_5$]-labeled N7-GA-Gua standard was added to each sample and filtered through an ultrafiltration membrane to remove DNA. The eluted-solution was evaporated thoroughly and dissolved in water, and then the solutions were subsequently quantified by LC/MS/MS.

RESULTS

Cytotoxicity and Genotoxicity of AA and GA Under Metabolic Activation

We used human microsomal preparation and phenobarbital- and 5,6-benzoflavone-treated rat liver S9 for metabolic activation. CYP2E1 activity of the human microsomal preparation was more than twice that of the rat liver S9 preparations (2,917 vs. 1,295 pmol/mg/min).

Figure 1 shows the cytotoxicity (RS; relative survival), MN, and *TK*-mutations induced by AA (a) and GA (b) with and without rat liver S9 or human microsomes. Rat liver S9 or human microsomes enhanced cytotoxicity (RS) of AA and GA. On the other hand, AA showed weak genotoxicity only at relatively high concentrations (>10 mM) without S9, but neither activating system enhanced the weak genotoxicty. GA induced TK-mutations dose-dependently from the low concentration (0.5 mM) and induced MN from 1.5 mM both with and without S9. Thus, neither the rat nor human metabolizing system activated AA or inhibited the expression of GA genotoxicity.

umu Assay Using Strains Expressing Human CYP2E1

We used *S. typhimurium* OY1002/2E1 strain to assess the cell toxicity and genotoxicity of AA at exposures up to 10mM (Fig. 2c). We also examined AA and GA with
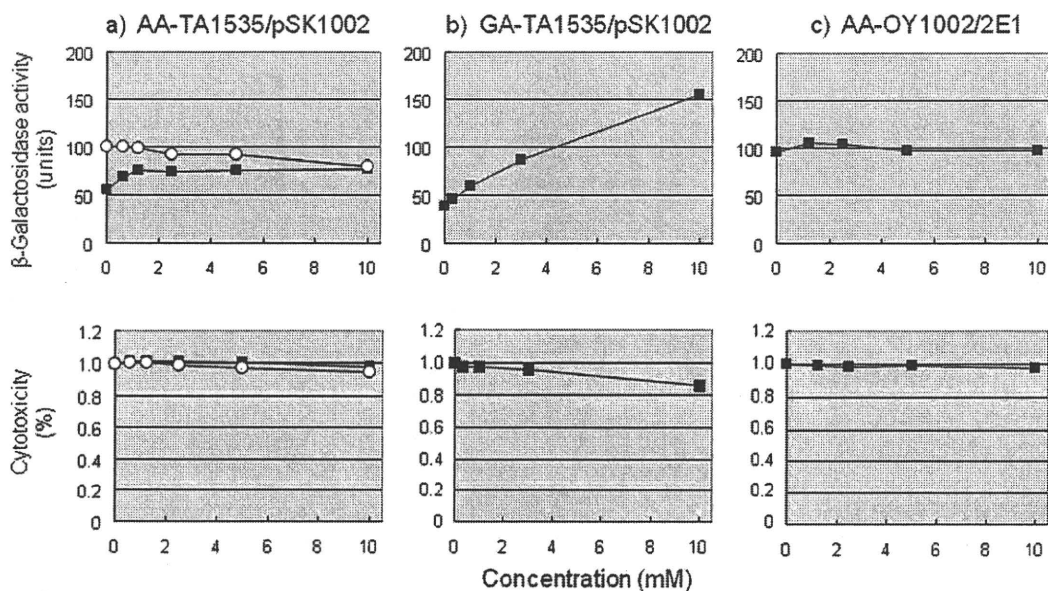
Environmental and Molecular Mutagenesis. DOI 10.1002/em

Genotoxicity of Acrylamide In Vitro   15

a) AA-TA1535/pSK1002   b) GA-TA1535/pSK1002   c) AA-OY1002/2E1

Fig. 2. Induction of *umuC* gene expression and cytotoxic response by AA (a, c) or GA (b) in *S. typhimurium* tester strains TA1535/pSK1002 (a, b) and OY1002/2E1 (c). The *umu* tests were conducted without (■) or with rat S9 (○). β-Galactosidase activity (units) was determined as described in Materials and Methods. Cytotoxic activities are expressed as % optical density change at 600 nm.

or without rat S9 using TA1535/pSK1002 strain. Although GA clearly produced a dose-related increase in response to DNA damage (Fig. 2b), AA elicited no genotoxic or cell toxic response with and without S9 (Fig. 2a). Thus, we could not demonstrate any in vitro genotoxicity of AA in the bacterial system.

Cytotoxic and Genotoxic Responses to AA in Transgenic Cell Lines

Western blot analysis revealed that h2E1v2 accumulated more CYP2E1 than either of its parental cell lines (Fig. 3). Both the h2E1v2 and AHH-1 cells exhibited weak responses (TK-gene mutations and MN) to AA at ≤3 mM with little difference in cytotoxicity (RSG, relative suspension growth) (Fig. 4a). h2E1v2 differed from AHH-1, however, in that it showed clear genotoxic and cytotoxic responses (RSG) to DMN, which is a representative substrate for CYP2E1 (Fig. 4b). Thus, the h2E1v2 cell line had CYP2E1 activity but did not activate AA.

DNA Adduct Formation by AA and GA in the Cell Lines

AA induced trace amounts of N7-GA-Gua adduct in TK6 cells (with and without S9) (Fig. 5a) and in AHH-1 and h2E1v2 cells (Fig. 5b). GA, on the other hand, induced a substantial number of N7-GA-Gua adducts in TK6 cells (Fig. 5c). These results suggest that the expression of genotoxicity may be dependent on N7-GA-Gua
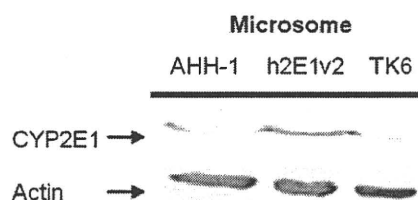

Fig. 3. Western blot analysis of CYP2E1 in AHH-1, h2E1v2, and TK6 cells. Equal amount of materials were loaded for each sample. CYP2E1 protein was stained with the anti-CYP2E1 antibody. Actin was used as a loading control.

adduct formation, and the in vitro metabolic activation system did not metabolize AA into GA.

DISCUSSION

A large number of studies about the in vitro genotoxicity of AA have been reported [Dearfield et al., 1995; Besaratinia and Pfeifer, 2005]. AA was negative in Ames assay in both the presence and absence of S9 [Zeiger et al., 1987; Knaap et al., 1988; Tsuda et al., 1993]. In mammalian cell assays, cytogenetic tests such as chromosome aberration test and sister chromatid exchange tests were positive [Sofuni et al., 1985; Tsuda et al., 1993]. AA also induced *Tk* mutation in the MLA but did not induce *Hprt* mutation in V79 cells [Moore et al., 1987;
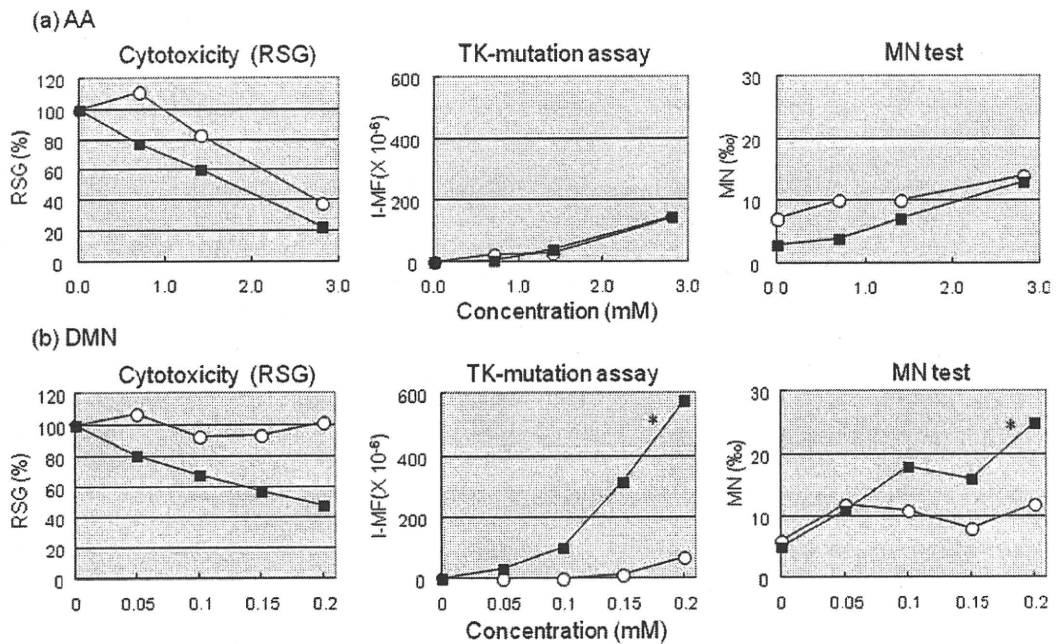
Fig. 4. Cytotoxic (relative suspension growth, RSG) and genotoxic (TK assay and MN test) responses of AHH-1 (○) or h2E1v2 (■) cells treated with AA or DMN for 4 hr. I-MF means induced mutation fraction, in which back ground mutation frequency is subtracted. *P < 0.05 (Omori method for TK-mutation assay, trend test for MN assay).

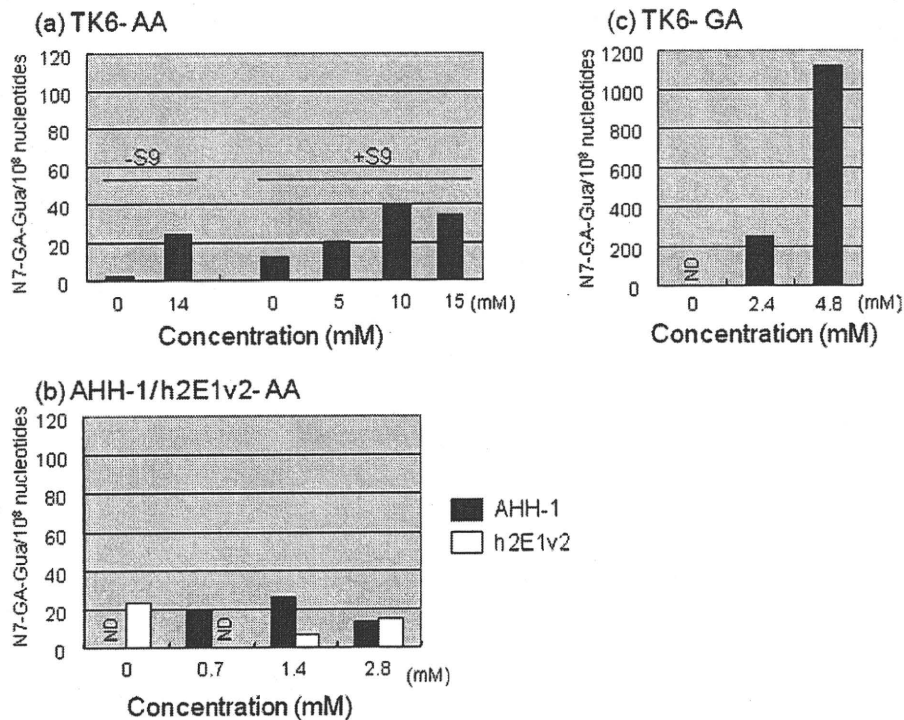
Fig. 5. Levels of N7-GA-Gua adduct in TK6 (a, c), AHH-1 (b), or h2E1v2 (b) cells treated with AA (a, b) or GA (c) for 4 hr at different concentrations. Data are expressed as the number of adducts in 10^8 nucleotides.

Environmental and Molecular Mutagenesis. DOI 10.1002/em

Genotoxicity of Acrylamide In Vitro   17

Knaap et al., 1988; Tsuda et al., 1993; Baum et al., 2005; Mei et al., 2008], and produced negative results in the Comet assay with V79 cells and human lymphocytes [Baum et al., 2005]. We also obtained positive results in TK gene mutation and micronuclei assays, but not in Comet assay using human lymphoblastoid TK6 cell in the absence of S9 [Koyama et al., 2006]. To obtain the positive results in the MLA and TK6 cells, however required very high dose of AA, which was sometimes beyond the top dose of the OECD testing guideline (>10 mM) [Koyama et al., 2006; Mei et al., 2008]. The spectrum of AA-induced TK mutations in TK6 and cII mutations in Big Blue[TM] mouse embryonic fibroblasts were not significantly different from the spontaneous one, although its metabolite GA distinctly induced a specific point mutation [Besaratinia and Pfeifer, 2003, 2004; Koyama et al., 2006]. Thus, the in vitro genotoxicity of AA is still controversial.

In contrast, the in vivo genotoxicity of AA has been clearly demonstrated by various rodent genotoxicity tests including micronuclei tests in peripheral blood [Cao et al., 1993; Abramsson-Zetterberg, 2003; Manjanatha et al., 2005], transgenic gene mutation in liver [Manjanatha et al., 2005], and Comet assay in various organs [Ghanayem et al., 2005b]. AA has also proven to be genotoxic to germ cells [Dearfield et al., 1995]. AA induced micronuclei in mice spermatids, and heritable chromosome translocations and specific locus mutations in postomeiotic sperm and spermatogonia [Lahdetie et al., 1994; Xiao and Tates, 1994]. AA also elevated the frequency of dominant lethal mutations probably accompanying with chromosome aberrations leading to death of embryo [Shelby et al., 1987; Adler et al., 1994]. The International Agency for Research on Cancer (IARC) classified it as 2A, a probable human carcinogen based on finding of rodent carcinogenicity [IARC, 1994]. AA caused tumors in various organs including mammary gland, peritesticular mesothelium, thyroid, and central nervous system [Carere, 2006], although the AA-inducing genotoxicity in these organs have not been demonstrated.

AA is metabolized either via direct glutathione conjugation followed by excretion of mercapturic acid or via oxidative pathways catalyzed by CYP2E1 to yield GA [Calleman et al., 1990; Wu et al., 1993; Sumner et al., 1999]. GA reacts quickly with DNA, mainly forming N7-GA-Gua adduct. Genotoxicity of GA has been demonstrated in vitro and in vivo. In contrast to AA, GA is positive in most genotoxicity tests [Hashimoto and Tanii, 1985; Dearfield et al., 1995; Besaratinia and Pfeifer, 2004; Baum et al., 2005; Koyama et al., 2006]. Manjanatha et al. [2005] demonstrated in transgenic Big Blue[TM] mice that both AA and GA induces endogenous Hprt and transgenic cII mutation at same level, and also produced similar mutational spectra. The predominant type of mutations observed in these two systems was G:C to T:A

transversion, which is presumably derived from N7-GA-Gua [Besaratinia and Pfeifer, 2005]. The in vivo results with transgenic Big Blue[TM] mice indicate that in vivo expression of AA genotoxicity is mediated via its GA metabolite.

However, no one has succeeded in demonstrating metabolically activated AA genotoxicity in vitro [Knaap et al., 1988; Tsuda et al., 1993; Dearfield et al., 1995; Friedman, 2003; Emmert et al., 2006]. In this study, we used induced rat liver S9 and human microsomal fraction for the metabolic activation. Although they have high CYP2E1 activity, the AA-inducing genotoxicity was never influenced by the presence of the exogenous metabolic activation system (Fig. 1a). We assumed that GA, a reactive epoxide, could be rapidly inactivated through microsomal epoxide hydrolase or glutathione in any S9 or microsomal fraction resulting in either the metabolism or the conjugation and detoxification of GA [Sumner et al., 2003; Decker et al., 2009]. However, presence of rat S9 did not prevent GA from inducing TK-mutation and micronuclei.

The umu assay could not detect the genotoxicity of AA even by the strain (Fig. 2). Emmert et al. [2006] also failed to demonstrate the mutagenicity of AA in the Ames test using the metabolically competent S. typhimurium strain YG7108pinERb₅ that expresses CYP2E1. In mammalian cell system, such as the human lymphoblastoid cell line, h2E1v2 overexpressing human CYP2E1 did not show different response in TK-gene mutation and MN induction compared to its parental cell line, AHH-1, although these cell lines exhibited distinct difference to DMN, which is a representative substrate for CYP2E1. We also investigated the genotoxicity of AA in h2E1v2 cells after long exposure (24 hr), because AA may be slowly metabolized to GA. The result was also negative (data not shown). Thus, we could not obtain any evidence of in vitro genotoxicity of AA via metabolic activation.

Glatt et al. [2005] developed a Chinese hamster V79-derived cell line that stably expresses human CYP2E1 and sulphotransferase (SULT), and applied it to investigate sister chromatid exchanges (SCE) induced by some chemicals. They demonstrated that AA induced SCE in the transgenic cell line but not in the parental line. Although the reason for the discrepancy between their results and ours is not clear, it is possible that another enzyme, such as SULT, may be involved in metabolic activation of AA.

The DNA adduct analysis clearly revealed that h2E1v2 cells does not generate N7-GA-Gua adduct in vitro. Because exposure of human cells to GA results in significant accumulation of N7-GA-Gua adduct, but DNA adduct analysis following exposure of h2E1v2 with AA does not generate N7-GA-Gua adduct in vitro, lead one a conclusion that the presence of CYP2E1 alone is not enough to metabolize AA to GA in mammalian cells. The

DNA adduct analysis also strongly supports a hypothesis that GA contribute to its genotoxicity by forming N7-GA-Gua adduct. Interestingly, very small amount of N7-GA-Gua adduct was generated in TK6 cells in a dose-dependent manner regardless of the presence of S9 (Fig. 5a). TK6 cells themselves may have an enzymatic activity to metabolize AA to GA, although its activity must be extremely low. Ghanayem et al. [2005b] showed that AA was not mutagenic or genotoxic in CYP2E1-null mice. Intraperitoneal injection of AA (25, 50 mg/kg) by once daily for 5 days induced micronuclei in erythrocyte and DNA damage assessed by Comet assay in leukocyte and liver cells of wild-type, but not in the CYP2E1-null mice. The plasma concentration of AA in the CYP2E1-null mice was 115-times higher than in the wild-type mice, while the GA concentration in the CYP2E1-null mice was negligible compared to that in the wild-type mice [Ghanayem et al., 2000]. Ghanayem et al. [2005c] also demonstrated that AA produces dominant lethal in mice that express CYP2E1, but not in mice that do not express CYP2E1, indicating that induction of germ cell mutations by AA in mice in vivo is also dependent upon CYP2E1 metabolism. These results clearly suggest that CYP2E1 is the principal enzyme responsible for the metabolism of AA to GA in vivo.

In conclusion, AA could not be metabolized to GA by in vitro metabolic activation system commonly used in genotoxicity tests. In vivo, on the other hand, GA is apparently responsible for AA-inducing genotoxicity. Although AA may exhibit genotoxicity in in vitro mammalian cells at high concentrations, its positive response is not relevant for its major genotoxicity. AA could be classified into in vivo specific genotoxic chemical.

ACKNOWLEDGMENT

REFERENCES

Abramsson-Zetterberg L. 2003. The dose-response relationship at very low doses of acrylamide is linear in the flow cytometer-based mouse micronucleus assay. Mutat Res 535:215–222.

Adler ID, Reitmeir P, Schmoller R, Schriever-Schwemmer G. 1994. Dose response for heritable translocations induced by acrylamide in spermatids of mice. Mutat Res 309:285–291.

Aryal P, Yoshikawa K, Terashita T, Guengerich FP, Shimada T, Oda Y. 1999. Development of a new genotoxicity test system with Salmonella typhimurium OY1001/1A2 expressing human CYP1A2 and NADPH-P450 reductase. Mutat Res 442:113–120.

Aryal P, Terashita T, Guengerich FP, Shimada T, Oda Y. 2000. Use of genetically engineered Salmonella typhimurium OY1002/1A2 strain coexpressing human cytochrome P450 1A2 and NADPH-cytochrome P450 reductase and bacterial O-acetyltransferase in SOS/umu assay. Environ Mol Mutagen 36:121–126.

Baum M, Fauth E, Fritzen S, Herrmann A, Mertes P, Merz K, Rudolphi M, Zankl H, Eisenbrand G. 2005. Acrylamide and glycidamide:

Genotoxic effects in V79-cells and human blood. Mutat Res 580:61–69.

Besaratinia A, Pfeifer GP. 2003. Weak yet distinct mutagenicity of acrylamide in mammalian cells. J Natl Cancer Inst 95:889–896.

Besaratinia A, Pfeifer GP. 2004. Genotoxicity of acrylamide and glycidamide. J Natl Cancer Inst 96:1023–1029.

Besaratinia A, Pfeifer GP. 2005. DNA adduction and mutagenic properties of acrylamide. Mutat Res 580:31–40.

Calleman CJ, Bergmark E, Costa LG. 1990. Acrylamide is metabolized to glycidamide in the rat: Evidence from hemoglobin adduct formation. Chem Res Toxicol 3:406–412.

Cao J, Beisker W, Nusse M, Adler ID. 1993. Flow cytometric detection of micronuclei induced by chemicals in poly- and normochromatic erythrocytes of mouse peripheral blood. Mutagen 8:533–541.

Carere A. 2006. Genotoxicity and carcinogenicity of acrylamide: A critical review. Ann Ist Super Sanita 42:144–155.

Crespi CL, Thilly WG. 1984. Assay for gene mutation in a human lymphoblast line, AHH-1, competent for xenobiotic metabolism. Mutat Res 128:221–230.

Crespi CL, Langenbach R, Penman BW. 1993a. Human cell lines, derived from AHH-1 TK+/- human lymphoblasts, genetically engineered for expression of cytochromes P450. Toxicology 82:89–104.

Crespi CL, Penman BW, Gonzalez FJ, Gelboin HV, Galvin M, Langenbach R. 1993b. Genetic toxicology using human cell lines expressing human P-450. Biochem Soc Trans 21:1023–1028.

Dearfield KL, Douglas GR, Ehling UH, Moore MM, Sega GA, Brusick DJ. 1995. Acrylamide: A review of its genotoxicity and an assessment of heritable genetic risk. Mutat Res 330:71–99.

Decker M, Arand M, Cronin A. 2009. Mammalian epoxide hydrolases in xenobiotic metabolism and signalling. Arch Toxicol 83:297–318.

Doerge DR, da Costa GG, McDaniel LP, Churchwell MI, Twaddle NC, Beland FA. 2005. DNA adducts derived from administration of acrylamide and glycidamide to mice and rats. Mutat Res 580:131–141.

Emmert B, Bunger J, Keuch K, Muller M, Emmert S, Hallier E, Westphal GA. 2006. Mutagenicity of cytochrome P450 2E1 substrates in the Ames test with the metabolic competent S. typhimurium strain YG7108pin3ERb5. Toxicology 228:66–76.

Friedman M. 2003. Chemistry, biochemistry, and safety of acrylamide. A review. J Agric Food Chem 51:4504–4526.

Furth EE, Thilly WG, Penman BW, Liber HL, Rand WM. 1981. Quantitative assay for mutation in diploid human lymphoblasts using microtiter plates. Anal Biochem 110:1–8.

Gamboa da Costa G, Churchwell MI, Hamilton LP, Von Tungeln LS, Beland FA, Marques MM, Doerge DR. 2003. DNA adduct formation from acrylamide via conversion to glycidamide in adult and neonatal mice. Chem Res Toxicol 16:1328–1337.

Ghanayem BI, Hoffler U. 2007. Investigation of xenobiotics metabolism, genotoxicity, and carcinogenicity using Cyp2e1(-/-) mice. Curr Drug Metab 8:728–749.

Ghanayem BI, Wang H, Sumner S. 2000. Using cytochrome P-450 gene knock-out mice to study chemical metabolism, toxicity, and carcinogenicity. Toxicol Pathol 28:839–850.

Ghanayem BI, McDaniel LP, Churchwell MI, Twaddle NC, Snyder R, Fennell TR, Doerge DR. 2005a. Role of CYP2E1 in the epoxidation of acrylamide to glycidamide and formation of DNA, hemoglobin adducts. Toxicol Sci 88:311–318.

Ghanayem BI, Witt KL, Kissling GE, Tice RR, Recio L. 2005b. Absence of acrylamide-induced genotoxicity in CYP2E1-null mice: Evidence consistent with a glycidamide-mediated effect. Mutat Res 578:284–297.

Ghanayem BI, Witt KL, El-Hadri L, Hoffler U, Kissling GE, Shelby MD, Bishop JB. 2005c. Comparison of germ cell mutagenicity in male CYP2E1-null and wild-type micetreated with acrylamide: Evidence supporting a glycidamide-mediated effect. Biol Reprod 72:157–163.

Environmental and Molecular Mutagenesis. DOI 10.1002/em

Genotoxicity of Acrylamide In Vitro   19

Glatt H, Schneider H, Liu Y. 2005. V79-hCYP2E1-hSULT1A1, a cell line for the sensitive detection of genotoxic effects induced by carbohydrate pyrolysis products and other food-borne chemicals. Mutat Res 580:41–52.

Hakura A, Shimada H, Nakajima M, Sui H, Kitamoto S, Suzuki S, Satoh T. 2005. Salmonella/human S9 mutagenicity test: A collaborative study with 58 compounds. Mutagen 20:217–228.

Hargreaves MB, Jones BC, Smith DA, Gescher A. 1994. Inhibition of p-nitrophenol hydroxylase in rat liver microsomes by small aromatic and heterocyclic molecules. Drug Metab Dispos 22: 806–810.

Hashimoto K, Tanii H. 1985. Mutagenicity of acrylamide and its analogues in Salmonella typhimurium. Mutat Res 158:129–133.

Honma M, Hayashi M, Sofuni T. 1997. Cytotoxic and mutagenic responses to X-rays and chemical mutagens in normal and p53-mutated human lymphoblastoid cells. Mutat Res 374:89–98.

IARC. Acrylamide. In:IARC Monographs on the Evaluation of Carcinogen Risk to Human: Some Industrial Chemicals, Vol. 60. Lyon: International Agency for Research on Cancer. Lyon. 1994. pp 389–433.

Ikeda T, Nishimura K, Taniguchi T. 2001. In vitro evaliation of drug interaction caused by enzyme inhibition-HAB protocol. Xenobiol Metabol Dispos 16:115–126.

Knaap AG, Kramers PG, Voogd CE, Bergkamp WG, Groot MG, Langebroek PG, Mout HC, van der Stel JJ, Verharen HW. 1988. Mutagenic activity of acrylamide in eukaryotic systems but not in bacteria. Mutagen 3:263–268.

Koyama N, Sakamoto H, Sakuraba M, Koizumi T, Takashima Y, Hayashi M, Matsufuji H, Yamagata K, Masuda S, Kinae N, Honma M. 2006. Genotoxicity of acrylamide and glycidamide in human lymphoblastoid TK6 cells. Mutat Res 603:151–158.

Lahdetie J, Suutari A, Sjoblom T. 1994. The spermatid micronucleus test with the dissection technique detects the germ cell mutagenicity of acrylamide in rat meiotic cells. Mutat Res 309:255–262.

Manjanatha MG, Aidoo A, Shelton SD, Bishop ME, MacDaniel LP, Doerge DR. 2005. Evaluation of mutagenicity in Big Blue (BB) mice administred acrylamide (AA) and glycidamide (GA) in drinking water for 4 weeks. Environ Mol Mutagen 44:214.

Matsushima T, Hayashi M, Matsuoka A, Ishidate M Jr, Miura KF, Shimizu H, Suzuki Y, Morimoto K, Ogura H, Mure K, Koshi K, Sofuni T. 1999. Validation study of the in vitro micronucleus test in a Chinese hamster lung cell line (CHL/IU). Mutagen 14:569–580.

Mei N, Hu J, Churchwell MI, Guo L, Moore MM, Doerge DR, Chen T. 2008. Genotoxic effects of acrylamide and glycidamide in mouse lymphoma cells. Food Chem. Toxicol 46:628–636.

Moore MM, Amtower A, Doerr C, Brock KH, Dearfield KL. 1987. Mutagenicity and clastogenicity of acrylamide in L5178Y mouse lymphoma cells. Environ Mutagen 9:261–267.

Mottram DS, Wedzicha BL, Dodson AT. 2002. Acrylamide is formed in the Maillard reaction. Nature 419:448–449.

Oda Y, Nakamura S, Oki I, Kato T, Shinagawa H. 1985. Evaluation of the new system (umu-test) for the detection of environmental mutagens and carcinogens. Mutat Res 147:219–229.

Oda Y, Aryal P, Terashita T, Gillam EM, Guengerich FP, Shimada T. 2001. Metabolic activation of heterocyclic amines and other pro-carcinogens in Salmonella typhimurium umu tester strains expressing human cytochrome P4501A1, 1A2, 1B1, 2C9, 2D6, 2E1, and 3A4 and human NADPH-P450 reductase and bacterial O-acetyltransferase. Mutat Res 492:81–90.

Omori T, Honma M, Hayashi M, Honda Y, Yoshimura I. 2002. A new statistical method for evaluation of L5178Ytk(+/−) mammalian cell mutation data using microwell method. Mutat Res 517:199–208.

Rice JM. 2005. The carcinogenicity of acrylamide. Mutat Res 580:3–20.

Sandhu P, Guo Z, Baba T, Martin MV, Tukey RH, Guengerich FP. 1994. Expression of modified human cytochrome P450 1A2 in Escherichia coli: Stabilization, purification, spectral characterization, and catalytic activities of the enzyme. Arch Biochem Biophys 309:168–177.

Segerback D, Calleman CJ, Schroeder JL, Costa LG, Faustman EM. 1995. Formation of N-7-(2-carbamoyl-2-hydroxyethyl)guanine in DNA of the mouse and the rat following intraperitoneal administration of [14C]acrylamide. Carcinogenesis 16:1161–1165.

Shelby MD, Cain KT, Cornett CV, Generoso WM. 1987. Acrylamide: Induction of heritable translocation in male mice. Environ Mutagen 9:363–368.

Sofuni T, Hayashi M, Matsuoka A, Sawada M. 1985. Mutagenicity tests on organic chemical concominants in city water and related compounds. II. Chromosome aberration tests in cultured mammalian cells. Eisei Shiken Hok 103:64–75.

Stadler RH, Blank I, Varga N, Robert F, Hau J, Guy PA, Robert MC, Riediker S. 2002. Acrylamide from Maillard reaction products. Nature 419:449–450.

Sumner SC, Fennell TR, Moore TA, Chanas B, Gonzalez F, Ghanayem BI. 1999. Role of cytochrome P450 2E1 in the metabolism of acrylamide and acrylonitrile in mice. Chem Res Toxicol 12:1110–1116.

Sumner SC, Williams CC, Snyder RW, Krol WL, Asgharian B, Fennell TR. 2003. Acrylamide: A comparison of metabolism and hemoglobin adducts in rodents following dermal, intraperitoneal, oral, or inhalation exposure. Toxicol Sci 75:260–270.

Suzuki S, Kurata N, Nishimura Y, Yasuhara H, Satoh T. 2000. Effects of imidazole antimycotics on the liver microsomal cytochrome P450 isoforms in rats: Comparison of in vitro and ex vivo studies. Eur J Drug Metab Pharmacokinet 25:121–126.

Tareke E, Rydberg P, Karlsson P, Eriksson S, Tornqvist M. 2000. Acrylamide: A cooking carcinogen? Chem Res Toxicol 13:517–522.

Tareke E, Rydberg P, Karlsson P, Eriksson S, Tornqvist M. 2002. Analysis of acrylamide, a carcinogen formed in heated foodstuffs. J Agric Food Chem 50:4998–5006.

Tornqvist M. 2005. Acrylamide in food: The discovery and its implications: A historical perspective. Adv Exp Med Biol 561:1–19.

Tsuda H, Shimizu CS, Taketomi MK, Hasegawa MM, Hamada A, Kawata KM, Inui N. 1993. Acrylamide; induction of DNA damage, chromosomal aberrations and cell transformation without gene mutations. Mutagen 8:23–29.

Wu YQ, Yu AR, Tang XY, Zhang J, Cui T. 1993. Determination of acrylamide metabolite, mercapturic acid by high performance liquid chromatography. Biomed Environ Sci 6:273–280.

Xiao Y, Tates AD. 1994. Increased frequencies of micronuclei in early spermatids of rats following exposure of young primary spermatocytes to acrylamide. Mutat Res 309:245–253.

Zeiger E, Anderson B, Haworth S, Lawlor T, Mortelmans K, Speck W. 1987. Salmonella mutagenicity tests. III. Results from the testing of 255 chemicals. Environ Mutagen 9(Suppl 9):1–109.